EFFECTS OF DELAYING EVAPORATOR FAN CYCLE OFF TIME FOR RESIDENTIAL AIR-CONDITIONING UNITS

 $ET11SCE1130\ Report$



Prepared by:

Design & Engineering Services Customer Service Business Unit Southern California Edison

March 20, 2012



Evaporator Fan Delay ET11SCE1130

Acknowledgements

Southern California Edison's Design & Engineering Services (DES) group is responsible for this project. It was developed as part of Southern California Edison's Emerging Technologies Program under internal project number ET11SCE1130. DES project manager, Rafik Sarhadian, PE, conducted this technology evaluation with overall guidance and management from Paul Delaney, Ramin Faramarzi, PE, and Henry Lau, PE, Ph.D. For more information on this project, contact Rafik.Sarhadian@sce.com.

Disclaimer

This report was prepared by Southern California Edison (SCE) and funded by California utility customers under the auspices of the California Public Utilities Commission. Reproduction or distribution of the whole or any part of the contents of this document without the express written permission of SCE is prohibited. This work was performed with reasonable care and in accordance with professional standards. However, neither SCE nor any entity performing the work pursuant to SCE's authority make any warranty or representation, expressed or implied, with regard to this report, the merchantability or fitness for a particular purpose of the results of the work, or any analyses, or conclusions contained in this report. The results reflected in the work are generally representative of operating conditions; however, the results in any other situation may vary depending upon particular operating conditions.

Evaporator Fan Delay ET11SCE1130

EXECUTIVE SUMMARY

This laboratory assessment investigated the potential energy efficiency benefits when evaporator fan cycle off time was delayed. The objective was achieved by testing a nominal 3-ton split air-conditioner under controlled environment conditions in the laboratory setting. The test unit was equipped with an air-cooled condenser and a single-speed compressor, which is one of the most common air-conditioning (A/C) units found in residential applications.

Normal operation of a typical residential A/C unit is such that when the thermostat setpoint temperature is met, both the compressor and evaporator (supply) fan cycle off. When the compressor and evaporator fan are cut off in response to the thermostat control, the evaporator coil is still partially flooded with the liquid refrigerant. This residual liquid refrigerant can be used to provide space cooling. This can occur by running the evaporator fan for a short time after the compressor cycles off. This period is referred to as "fan delay time, or period". While used for decades in residential space heating, it has not yet been fully evaluated in cooling applications. Fan delay technologies are commercially available for cooling applications either as an on-board by original equipment manufacturers, or as an add-on option.

This study involved conducting ten test scenarios at Southern California Edison's (SCEs) Technology Test Centers (TTC). The duration of each test was one hour. For every test scenario, the thermostat in the indoor test chamber (room) was set to 75 degrees Fahrenheit (°F) while the outdoor test chamber (ambient) was maintained at 115°F. Evaluation of various fan delay periods occurred under part load ratios (PLRs) of 0.34, 0.53, and 0.76. PLR is defined as the ratio of imposed cooling load in the room to cooling capacity of the A/C unit as published by the manufacturer for a particular outdoor/indoor condition. This led to identifying fan delay periods with the highest energy efficiency potential. In addition, it established variations in energy efficiency potentials as a function of PLRs.

This project evaluated two types of commercially available add-on delay controllers. One controller was capable of delaying fan cycle off period based on a prescribed time. The other controller had a built-in logic to delay the fan cycle off period based on the compressor's run time history. The control logic of the latter technology directly correlated fan delay periods with compressor run times.

Results obtained from these tests were later used to determine the equivalent electrical energy that was mitigated during fan delay periods. The equivalent electrical energy was determined as a function of the amount of heat extracted from the evaporator coil during fan delay periods. After a close review of findings, three optimum test scenarios were identified. It should be emphasized that project findings and conclusions are specific to the particular 3-ton unit tested.

Project findings indicated delaying the evaporator fan cycle off time had no impact on the overall power demand of the tested A/C unit. Electrical energy savings potentials, on the other hand, noticeably varied as a function of delay periods and PLRs. For optimum delay periods of four to five minutes, as the PLR increased from 0.34 to 0.76, the energy savings reduced from 20.6% to 4.5%. Clearly, at 100% PLR the energy savings diminished. The A/C units with single-speed compressor typically operate at full capacity even during periods when cooling load in the conditioned space is less than the A/C unit's cooling capacity. Under such conditions, while the compressor may operate at full load without substantial variations in power demand, its run time will be decreased.

Evaporator Fan Delay ET11SCE1130

The project findings coupled with building energy simulation results can be used to establish annual energy savings. Subsequently, the eQUEST building energy simulation modeling was performed for a two story residential home. The A/C unit for the model home was a 3.5-ton split system with a seasonal energy efficiency ratio of 13. The conditioned space was 1,768 square feet. The simulation was done for all 16 climate zones. The key variables from the hourly simulation report were extracted and combined with the test findings to calculate the annual energy savings. Results are summarizes in Table 1. To establish the annual energy savings for different building characteristics including vintages and sizes, it is recommended to repeat the same methodology.

TABLE 1. ANNUAL COOLING ENERGY CONSUMPTION AND SAVINGS IN ALL 16 CLIMATE ZONES			
CLIMATE ZONE	ANNUAL COOLING ENERGY CONSUMPTION (KWH/YR)	Annual Cooling Energy Savings (KWH/YR)	
1	100	28	
2	2,052	324	
3	742	184	
4	1,835	331	
5	1,157	236	
6	1,199	293	
7	1,540	323	
8	2,526	425	
9	2,964	454	
10	3,599	490	
11	3,363	383	
12	2,804	373	
13	4,762	501	
14	4,264	431	
15	9,021	814	
16	1,181	187	

ABBREVIATIONS AND ACRONYMS

A/C	Air-Conditioning		
AHRI	Air-Conditioning, Heating, and Refrigeration Institute		
ASHRAE	American Society of Heating, Refrigerating and Air-Conditioning Engineers		
Btu	British Thermal Unit		
cfm	Cubic-feet-per-minute		
CZ	Climate Zone		
DBT	Dry-Bulb Temperature		
DPT	Dew-Point Temperature		
EER	Energy Efficiency Ratio		
fpm	Feet-per-minute		
FS	Full Scale		
kW	Kilowatt		
PLR	Part Load Ratio		
RH	Relative Humidity		
RmSHR	Room (indoor test chamber) Sensible Heat Ratio		
SCE	Southern California Edison		
SHR	Sensible Heat Ratio		
ттс	Technology Test Centers		
W	Watt		
WBT	Wet-Bulb Temperature		

CONTENTS

XECUTIVE SUMMARY	I
ITRODUCTION	_ 1
ACKGROUND	_ 2
ESCRIPTION OF FAN DELAY TECHNOLOGY	_ 3
est Design	_ 4
Test Unit4	
Test Methodology5	
Air-Enthalpy Method5 Refrigerant-Enthalpy Method5	
Monitoring Points6	
Data Acquisition7	
ESULTS	8
Power and Energy8	
Energy Efficiency Ratios12	
Heat Extraction Rate During Fan Delay Period12	
Net Energy Benefit During Fan Delay Period13	
Energy Savings Potential14	
Estimating Annual Energy Savings15	
ONCLUSIONS	_ 17
ECOMMENDATIONS	_ 18
PPENDIX A – INSTRUMENTATION	_ 19
PPENDIX B – ENGINEERING CALCULATIONS	_ 20
Gross and Net Cooling Capacity	

APPENDIX C - MEASUREMENT UNCERTAINTY	_ 26
Quantify Components of Standard Uncertainties for a Single	
Measurement	
Calculate the Expanded Uncertainty29	
APPENDIX D – TEST SCENARIOS AND PRELIMINARY RESULTS	_ 31
Test Scenarios31	
Selected Test Scenarios for Analysis	
Part Load Ratios Corresponding to Test Scenarios34	
Indoor (room) and Outdoor (ambient) Conditions35	
Comparison of Gross (total) Cooling Rate37	
APPENDIX E – HOURLY SIMULATION REPORT	_ 39
APPENDIX F – TECHNOLOGY TEST CENTERS	_ 40
Heating, Ventilation, and Air Conditioning Technology Test Center40	
Responsibilities	
REFERENCES	42

FIGURES

Figure 1.	Photograph of Fan Delay Controllers3
Figure 2.	Picture of the Indoor Section of the Air-Conditioning Unit in the Indoor Test Chamber4
Figure 3.	Schematic Diagram of Test Setup with Monitoring Points7
Figure 4.	One-Minute Profile of Compressor and Evaporator Fan Power [0.9 ton test scenario]8
Figure 5.	One-Minute Profile of Compressor and Evaporator Fan Power [1.3 ton test scenario]9
Figure 6.	One-Minute Profile of Compressor and Evaporator Fan Power [1.8 ton test scenario]10
Figure 7.	Total, Compressor, and Evaporator Fan Average Power 11 $$
Figure 8.	Total, Compressor, and Evaporator Fan Energy11
Figure 9.	Net and Net Sensible Energy Efficiency Ratio [airenthalpy method]12
Figure 10.	One-Minute Profile of Heat Extraction Rate During Fan Delay Period [air-enthalpy method]13
Figure 11.	Energy Savings Potential as a Function of Part Load Ratios
Figure 12.	Graphical Presentation of an Optimum Fan Delay Period . 33
Figure 13.	One-Minute Profile of Indoor (room) and Outdoor (ambient) Dry-Bulb Temperatures36
Figure 14.	Average Indoor (room) Wet-Bulb Temperature and Relative Humidity36
Figure 15.	Indoor (room) Dry-Bulb Temperature and Relative Humidity During one Complete Cycle [0.9 ton test scenario]
Figure 16.	Average Gross (total) Cooling Rate – Air- and Refrigerant-Enthalpy Methods

TABLES

Table 1.	Annual Cooling Energy Consumption and Savings in all 16 Climate Zones	ii
Table 2.	Summary of Net Energy Benefits (during one-hour test periods only)	14
Table 3.	Summary of Energy Savings Potential (during one-hour test periods only)	14
Table 4.	Annual Cooling Energy Savings in all 16 Climate Zones – Single Family Residence	16
Table 5.	Specifications, Calibration Dates, Locations, and Corresponding Monitoring Points for Sensors	19
Table 6.	Summary of All Test Scenarios	32
Table 7.	Imposed Cooling Load in the Indoor Test Chamber (room) and the Corresponding Sensible Heat Ratio	34
Table 8.	Part Load Ratio	35

EQUATIONS

Equation 1.G	ross Cooling Capacity (air-enthalpy method)	20
Equation 2.G	ross Cooling Capacity (refrigerant-enthalpy method)	21
Equation 3.N	et Cooling Capacity (air-enthalpy method)	21
Equation 4.G	ross Sensible Cooling Capacity (air-enthalpy method)	22
Equation 5.N	et Sensible Cooling Capacity (air-enthalpy method)	22
Equation 6.S	ensible heat Ratio (air-enthalpy method)	22
Equation 7.P	art Load Ratio	23
Equation 8.N	et Energy Efficiency Ratio (air-enthalpy method)	23
	et Sensible Energy Efficiency Ratio (air-enthalpy nethod)	24
Equation 10.	Evaporator Coil Superheat	24
Equation 11.	Condenser Coil Sub-cooling	24
Equation 12.	Total Air-Conditioning Unit Power	25
Equation 13.	Energy Usage	25
•	Standard Uncertainty with Sensor Specifications rectangular and triangular distributions)	26

	tandard deviation of mean)	. 27
•	Combined Standard Uncertainty for a Single easurement	. 28
•	General Equation for Combining Standard ncertainties [non-correlated quantities]	. 28
	Combined Standard Uncertainty for Equations volving Sums or Differences	. 29
	Combined Standard Uncertainty for Equations volving Products or Quotients	. 29
Equation 20.	Expanded Standard Uncertainty	. 30

INTRODUCTION

Typical residential furnaces run blowers (fans) for a period after the burner shuts off to extract the heat stored in the heat exchanger. Such practice, however, is not applied to the air-conditioning (A/C) units, although could be applied to "extract cooling" from the A/C units.

Ordinary operation of a typical A/C unit is such that when the room thermostat setpoint minus the throttling temperature is met, the A/C compressor cycles off and subsequently the evaporator fan cycles off. Typical A/C units have a built-in anti-short cycle timer to protect the compressor. For example, if the temperature setpoint is 75 degrees Fahrenheit (°F) with a throttling range of \pm 1°F, the compressor turns on when the temperature reaches 76°F and turns off at 74°F. Nonetheless, when the compressor shuts off in a response to the thermostat control, the evaporator coil is still partially flooded with liquid refrigerant. Ideally, the available cooling effect left in the liquid refrigerant can be used to provide space cooling. This can be done by running the evaporator fan for a short period after the compressor cycles off. The period where the evaporator fan continues running after the compressor cycles off is referred to as "fan delay time, or period".

The objectives of this laboratory assessment project were to evaluate the feasibility and the potential electrical demand and energy savings due to fan delay periods for a residential A/C unit. The assessment involved testing a 3-ton residential split-type A/C unit under a single outdoor ambient condition of 115°F. A 3-ton split unit is the most common A/C unit found in residential applications. Testing was performed for different fan delay periods under similar cooling load conditions, and for various cooling load levels. This project was conducted at Southern California Edison's (SCE's) Technology Test Centers (TTC) controlled environment chambers. Appendix F describes TTC's controlled environment test chambers.

Delaying evaporator fan cycle off time can be achieved either at the manufacturer level (new A/C units), or by retrofitting the existing A/C units by installing add-on controllers. In this project, two types of add-on controllers or devices were used. One controller allowed the user to set the time delay period. The other controller had a built-in logic to delay the fan cycle off period based on the compressor run time. The governing logic of this controller was the longer the compressor run time, the longer the fan delay period. Even though two types of controllers were used in this project, the key issue addressed here was the benefits and/or penalties realized for running the evaporator fan during fan delay periods.

BACKGROUND

The split A/C unit consists of two main fan coil units, one indoor and one outdoor. The indoor unit is comprised of the evaporator (cooling) coil, evaporator fan, and the furnace (heating) section. The outdoor (condensing) unit is comprised of the compressor, condenser coil, and the condenser fan. As their names imply, the indoor unit is installed either in the attic area, in a mechanical closet, or in the garage. Installation of the outdoor unit outdoors rejects heat to the ambient.

For typical residential A/C systems, the evaporator fan cycles off with the compressor when the thermostat setpoint is satisfied. After the compressor cycles off, the flow of refrigerant stops and some of this relatively cold refrigerant remains in the evaporator coil. In principle, to take advantage of the cooling capacity left in the evaporator coil, the evaporator fan can continue running to provide additional cooling to the conditioned space. That is, after the compressor stops running, the evaporator fan continues running to circulate the indoor air across the evaporator coil to provide additional sensible cooling.

Conceptually, additional sensible cooling provided during the fan delay period postpones the start of the next cooling cycle. The obvious penalty associated with providing this additional cooling is increased run time of the evaporator fan, or fan energy usage. So, from an energy standpoint, the benefits of the fan delay strategy is realized when the fan energy usage does not exceed the amount of space cooling, in terms of electrical energy, during fan delay periods.

DESCRIPTION OF FAN DELAY TECHNOLOGY

Assessment of the technology in a laboratory setting allowed evaluating the benefits of delaying different fan cycle off periods under various part load conditions while maintaining an identical thermostat setpoint. Clearly, cycling patterns will differ based on the type of residence (single-family, multi-family, mobile home), vintage, and quality of installation (leakiness affects cycling rates), capacity of the A/C unit, cooling load of the building, users preferred thermostat setpoint, ambient conditions, and time of day and year. Therefore, to estimate potential savings as a function of cycling patterns of the actual units in the field, field assessments may be needed beyond the laboratory testing.

The assessment started with running the A/C unit for different fan cycle off delay periods under an identical cooling load condition imposed in the indoor test chamber. The test duration for each cycle off delay period was one hour. Testing was repeated for different cooling loads while maintaining the same test durations and cycle off delay periods. Test scenarios are discussed in the Appendix D of this report.

Figure 1 shows a photograph of both controllers. The left photograph is the controller that allows the user to set the time delay period. The right photograph is the controller that has a built-in logic to delay the fan cycle off period based on the compressor run time.





FIGURE 1. PHOTOGRAPH OF FAN DELAY CONTROLLERS

TEST DESIGN

This section provides information on the test unit and protocols. It also addresses test design including key monitoring points and the data acquisition system.

TEST UNIT

The test unit installed in the test chambers of TTC was a 3-ton split system equipped with an air-cooled condenser and a single-speed compressor. Prior to any tests, the A/C system was charged with the proper amount of refrigerant (R-410A) following the manufacturer's instructions. Figure 2 shows a picture of the indoor section of the A/C unit installed in the indoor test chamber. The following lists the model numbers for the main component of the A/C unit under test.

Outdoor condensing unit: 4TTB3036D1000A,

refrigerant R-410A, nominal 3-ton

• Indoor coil: 4TXCB042B3, nominal 3-ton

• Gas furnace (blower unit): TUD1B080A9361A, 4-speed direct blower drive



FIGURE 2. PICTURE OF THE INDOOR SECTION OF THE AIR-CONDITIONING UNIT IN THE INDOOR TEST CHAMBER

TEST METHODOLOGY

The test unit's capacities and performance characteristics were determined following the American Society of Heating, Refrigerating, and Air-Conditioning Engineers (ASHRAE) Standard 37-2009,¹ and the Air-Conditioning, Heating, and Refrigeration Institute (AHRI) Standard 210/240.² The air- and refrigerant-enthalpy methods described by these test standards were used to measure psychrometric properties of the air and refrigerant properties. This involved installing instrumentation at specified locations as outlined by these standards. The air and refrigerant properties were used to determine the cooling capacities and efficiencies of the A/C unit at full load. However, at part load, the indoor and outdoor conditions deviated from those specified by test protocols. Discussions on the indoor and outdoor conditions appear in the Appendix D of this report.

Power measurements included input to compressor, condenser, and evaporator fan, and controls and other items required as part of the system for normal operation. Following test standards, air velocity near the installed unit was monitored to ensure it was maintained below 500 feet-per-minute (fpm). Additionally, the outdoor control environment room's 10-foot high ceiling provided sufficient clearance (more than the required six feet) from condenser discharge. The required distance of at least three feet was provided between the test room's walls and the equipment side surfaces. The following highlights the key aspects of air- and refrigerant-enthalpy methods.

AIR-ENTHALPY METHOD

The air-enthalpy method used measured psychrometric properties of air flowing across the A/C unit's evaporator coil. These measurements included dry-bulb temperature (DBT), wet-bulb temperature (WBT), and the relative humidity (RH) of air in the upstream and downstream of the coil at measured airflow rates. Accordingly, the air enthalpy change and airflow rate were used to determine the gross cooling capacity of the unit. Using the measured evaporator fan power input, the net cooling capacity of the unit was determined. This was done by subtracting evaporator fan heat from the gross cooling capacity.

REFRIGERANT-ENTHALPY METHOD

The refrigerant-enthalpy method used measured refrigerant properties at the inlet and outlet of the evaporator coil. The gross cooling capacity of the unit was determined using the refrigerant enthalpy change, and mass flow rate. Refrigerant enthalpy changes were determined from pressure and temperature measurements entering and leaving evaporator coil. A corriolis mass flow meter was installed in the liquid line to measure the liquid refrigerant flow rate. To obtain reliable refrigerant flow rate, the refrigerant must be in a 100% liquid state. Pressure transducers were installed before and after the mass flow meter to measure and record the pressure drop across the flow meter. Monitoring the pressure drop across the meter ensured that liquid refrigerant did not flash and undergo a saturation temperature change of larger than 3°F, as prescribed by the test standards. In addition, installation of two sight glasses immediately upstream and downstream of the flow meter confirmed the refrigerant was in a 100% liquid state at the inlet and outlet of the flow meter. In addition, measurements occurred for the temperature and pressure of the refrigerant vapor entering and leaving the compressor in the refrigerant lines approximately 10 inches from the compressor shell.

MONITORING POINTS

The monitoring plan included 94 points. The following list captures the core monitoring points. Figure 3, not to scale, depicts the schematic diagram of all sensor locations used in this project. As depicted, for critical temperature measurements including air entering and leaving the indoor unit, a temperature grid was assembled.

1. Refrigerant side

- Compressor discharge temperature and pressure
- Compressor suction temperature and pressure
- Liquid line temperature and pressure before and after the mass flow meter
- Refrigerant mass flow rate

2. Indoor air

- DBT
- WBT
- RH

3. Outdoor air

- DBT
- RH

4. Indoor unit

- Air DBT at the inlet of evaporator fan
- Air DBT and dew-point temperature (DPT) at the inlet of evaporator coil
- Air DBT, DPT, and RH at the outlet of evaporator fan

5. Condensate mass (using digital scale)

6. Power

- Compressor
- Condenser fan
- Evaporator fan
- Total indoor unit
- Total condensing (outdoor) unit
- Auxiliary heaters for indoor test chamber sensible load

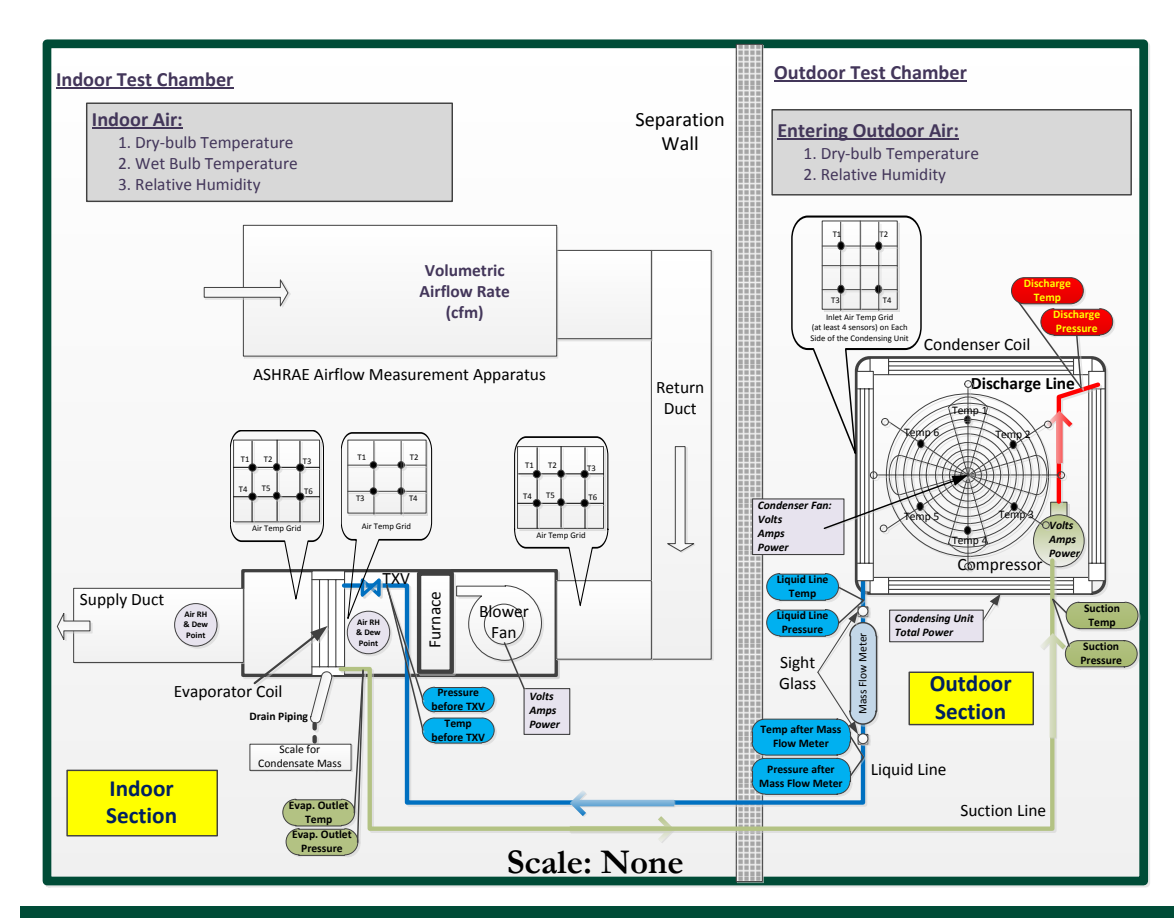


FIGURE 3. SCHEMATIC DIAGRAM OF TEST SETUP WITH MONITORING POINTS

DATA ACQUISITION

The logging of test data occurred by using the National Instruments' SCXI data acquisition system. The data acquisition system was set up to scan 94 data channels in 20-second intervals and log data in one-minute intervals. As part of TTCs quality control protocol, the design of the data acquisition system is completely independent of the supervisory control computer. This approach eliminated compromising the data collection by the control sequence's priority over data acquisition.

Screening of collected data ensured key control parameters were within the acceptable ranges. In the event that any of the control parameters fell outside the acceptable limits, the problem was flagged and a series of diagnostic investigations were carried out. Corrections were then made and tests were repeated, as necessary. After the data passed the initial screening process, data imported to a customized refrigeration analysis model where detailed calculations were performed (outlined in Appendix B). Appendix A lists the specifications for the instruments.

RESULTS

This section discusses results obtained from three selected test scenarios. Discussions on the engineering and measurement uncertainty calculations are in Appendices B and C, respectively. Appendix D details all test scenarios and preliminary results.

POWER AND ENERGY

Figure 4 illustrates a one-minute profile of compressor and evaporator fan power input, in watts (W), for a 0.9-ton test scenario over a 59-minute of data collection period. Testing observed six complete cycles. The cooling period for every complete cycle was three or four minutes. The fan delay period for every complete cycle was five minutes. The cycle off period for every complete cycle was one or two minutes. During the entire 59 minutes, the total cooling period was 21 minutes, total fan delay period was 30 minutes, and the total cycle off period was 8 minutes. For every cycle, as the cooling period continued, compressor power declined from 3,300W to 3,200W. Evaporator fan power was lower during fan delay periods compared to cooling periods. This indicated that the evaporator coil was dry and the static pressure drop across the dry coil was reduced.

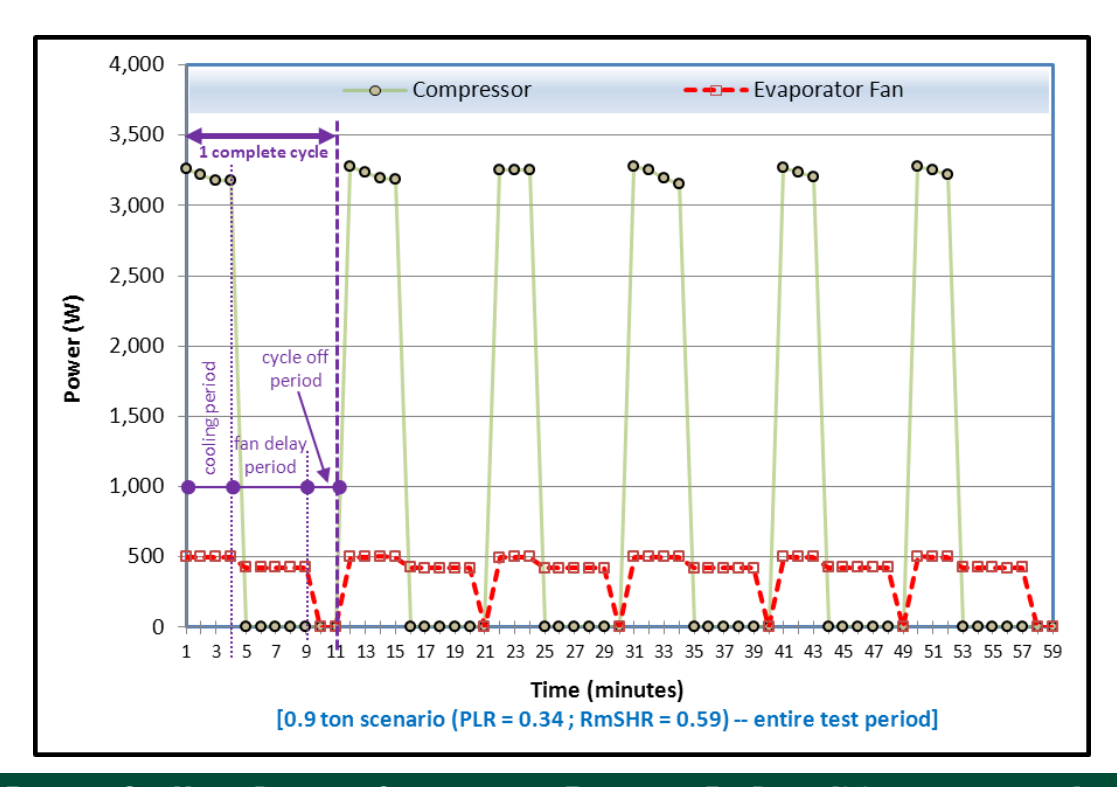


FIGURE 4. ONE-MINUTE PROFILE OF COMPRESSOR AND EVAPORATOR FAN POWER [0.9 TON TEST SCENARIO]

Figure 5 depicts a one-minute profile of the compressor and evaporator fan power input for a 1.3-ton test scenario over a 60-minute of data collection period. Testing observed six complete cycles. The cooling period for every complete cycle was either five, six, or seven minutes. The fan delay period for every complete cycle was four minutes. Since the system called for cooling after being in fan delay mode for four minutes, testing detected no cycle off period. During the entire 60 minutes, a total cooling and fan delay period was 36 and 24 minutes, respectively. For every cycle, as the cooling period continued, compressor power declined from 3,300W to 3,100W. As a result of partially wet coil just before the initiation of the fan delay period, evaporator fan power was slightly higher (by less than 30W) in the first minute relative to the last three minutes. Lower fan power during the last three minutes indicated that the evaporator coil was dry, which reduced the static pressure drop across the dry coil.

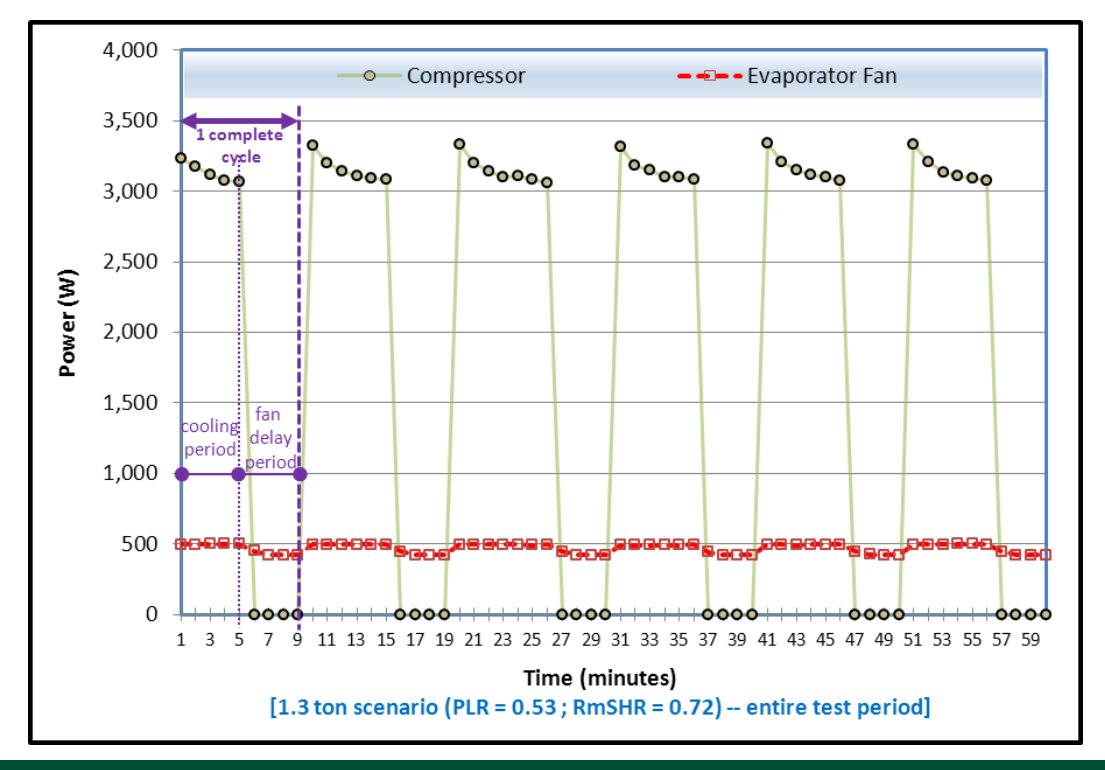


FIGURE 5. ONE-MINUTE PROFILE OF COMPRESSOR AND EVAPORATOR FAN POWER [1.3 TON TEST SCENARIO]

Figure 6 shows a one-minute profile of the compressor and evaporator fan power input for a 1.8-ton test scenario over a 60-minute period of data collection. Testing observed two complete cycles. The cooling period for the first and second cycle was 27 and 25 minutes, respectively. The fan delay period for every complete cycle was four minutes. Since the system called for cooling after being in fan delay mode for four minutes, testing detected no cycle off period. During the entire 60 minutes of testing, the total cooling period was 52 minutes and the total fan delay period was 8 minutes. Compressor power at the initiation of every cooling period was about 3,300W. As the cooling period continued, compressor power decreased and stayed at the 3,000W level until the end of the cooling period. Because of partially wet coil just before the initiation of the fan delay period, the evaporator fan power was slightly higher (by less than 30W) in the first minute relative to the last three minutes.

Lower fan power during the last three minutes indicated the evaporator coil was dry and the static pressure drop across the dry coil was reduced.

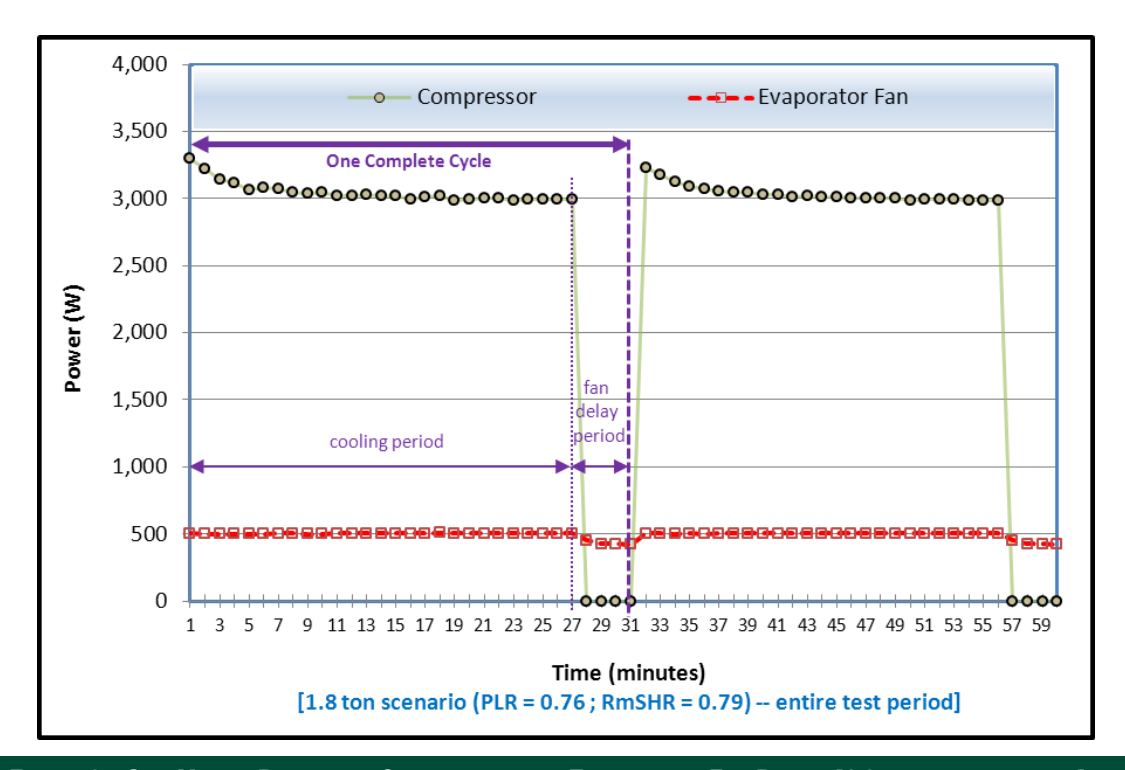


FIGURE 6. ONE-MINUTE PROFILE OF COMPRESSOR AND EVAPORATOR FAN POWER [1.8 TON TEST SCENARIO]

Figure 7 summarizes average total power during cooling periods, compressor power, and evaporator fan power during both cooling and fan delay periods. Corresponding uncertainties with each measurement (after \pm symbol) also display in Figure 7. The average total power during cooling periods combines both the indoor (evaporator fan and electronic boards) and outdoor section (compressor and condenser fan). Since the compressor was the major contributor to the total power, variations in compressor power directly reflected in total power. As the cooling load in the indoor test chamber increased from 0.9 to 1.8 tons, the average compressor power decreased. This was attributed to longer run times under increased cooling load conditions. The average evaporator fan power during both cooling and fan delay periods remained moderately unaffected by cooling load variations.

Figure 8 summarizes total energy during cooling period, compressor energy, and evaporator fan energy during both cooling and fan delay period. As the cooling load in the indoor test chamber increased from 0.9 to 1.8 tons, compressor energy and accordingly total energy usage increased. This was attributed to longer run times under increased cooling load conditions. In effect, as part load ratio (PLR) increased, the amount of time the system was in cooling mode also increased. This resulted in less available time for fan delay periods. Consequently, fan energy usage was lower during fan delay periods under increased cooling load conditions, or PLRs.

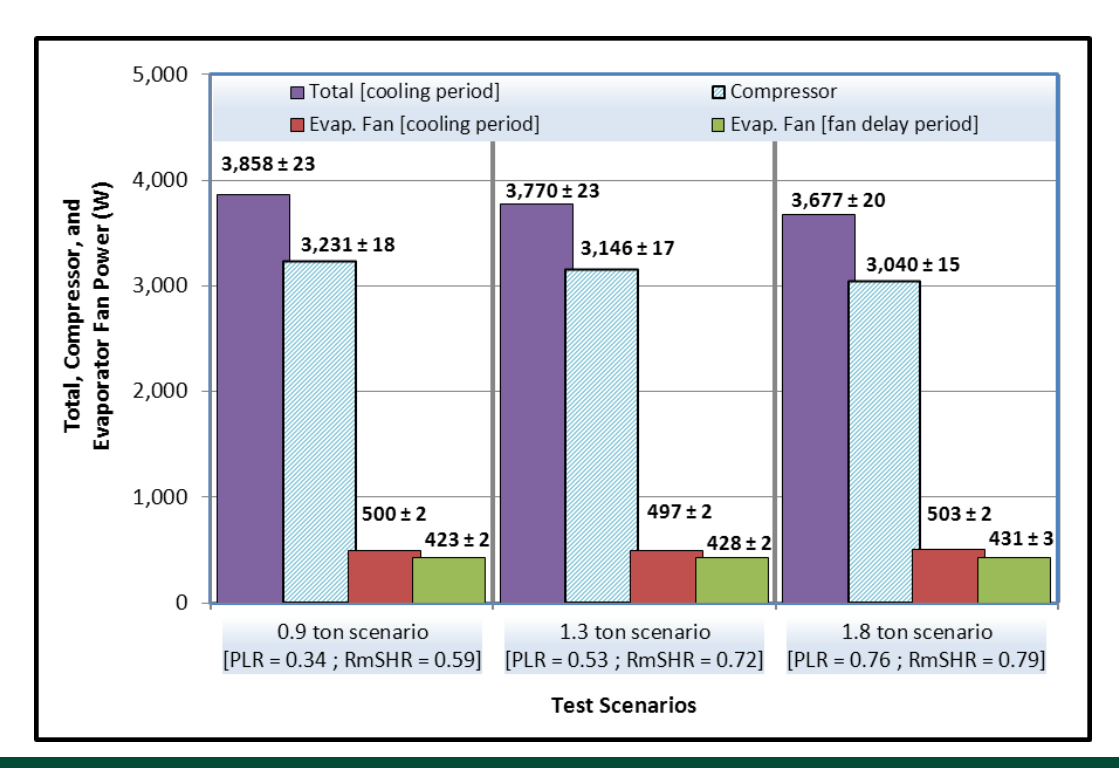


FIGURE 7. TOTAL, COMPRESSOR, AND EVAPORATOR FAN AVERAGE POWER

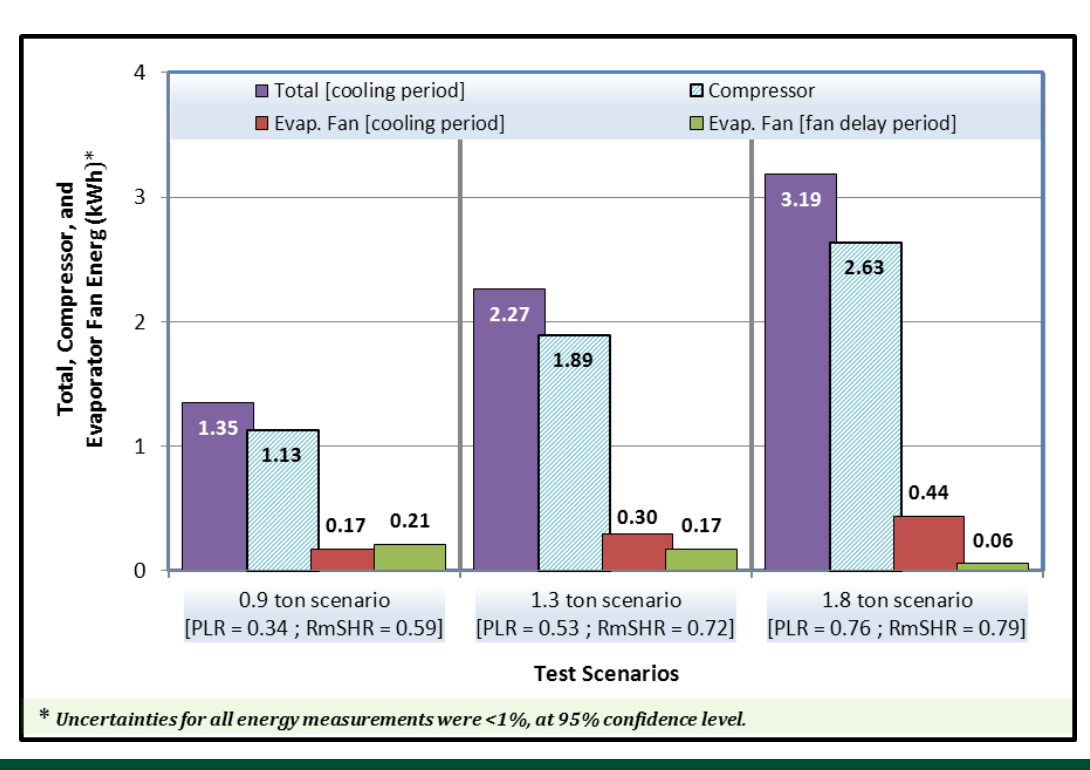


FIGURE 8. TOTAL, COMPRESSOR, AND EVAPORATOR FAN ENERGY

ENERGY EFFICIENCY RATIOS

Figure 9 summarizes both the net and net sensible energy efficiency ratio (EER) values with corresponding uncertainties (after \pm symbol). The EER values are in British thermal unit per hour per watts (Btu/hr/W). As the cooling load in the indoor test chamber increased from 0.9 to 1.8 tons, the net EER of the unit decreased. This was due to a reduction in the net cooling rate and the total power input. Conversely, as the cooling load increased from 0.9 to 1.8 tons, the net sensible EER increased. This was due to an increase in net sensible cooling rate relative to the reduction in total power input.

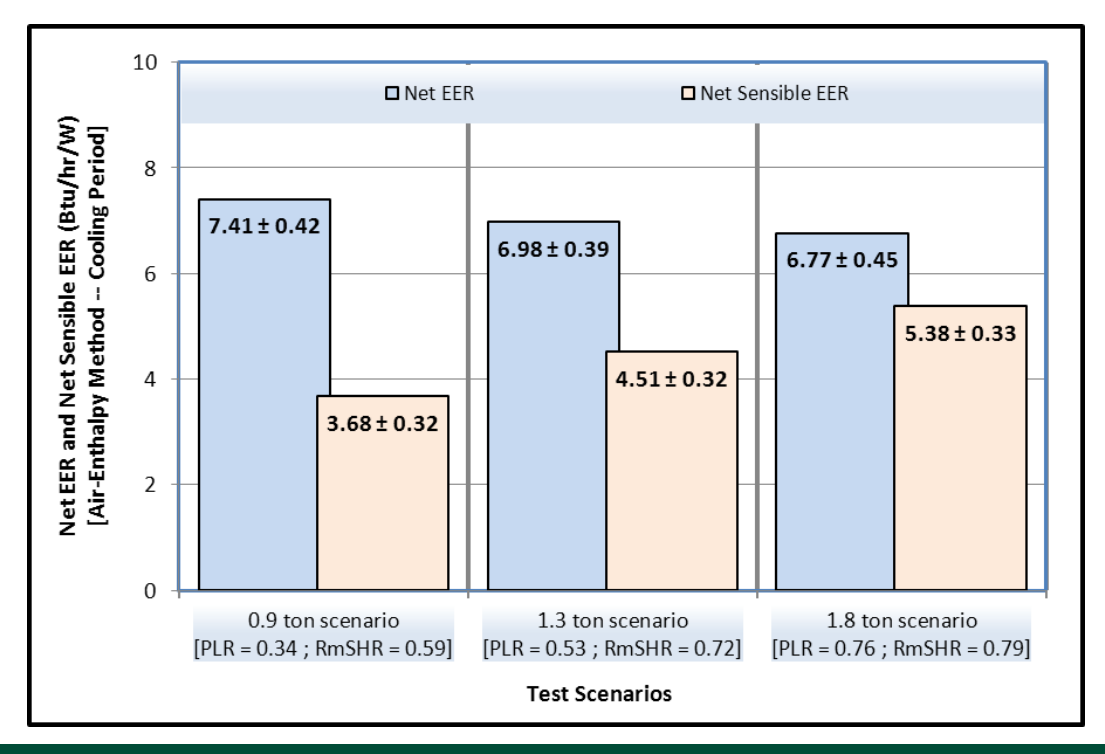


FIGURE 9. NET AND NET SENSIBLE ENERGY EFFICIENCY RATIO [AIR-ENTHALPY METHOD]

HEAT EXTRACTION RATE DURING FAN DELAY PERIOD

Figure 10 depicts a one-minute profile of heat extraction rate during fan delay periods. It signifies the liquid refrigerant's ability to remove heat per unit of time during fan delay periods. For each of the three selected test runs, the heat extraction profile during each complete cycle was relatively alike. Under higher PLR, the heat extraction rate was higher due to longer compressor run time and subsequently, operations at lower evaporating temperatures. For the 1.8-ton scenario, nonetheless, due to a reduction in the number of cycles and thereby total fan delay time, the aggregate heat extracted during fan delay periods was the lowest.

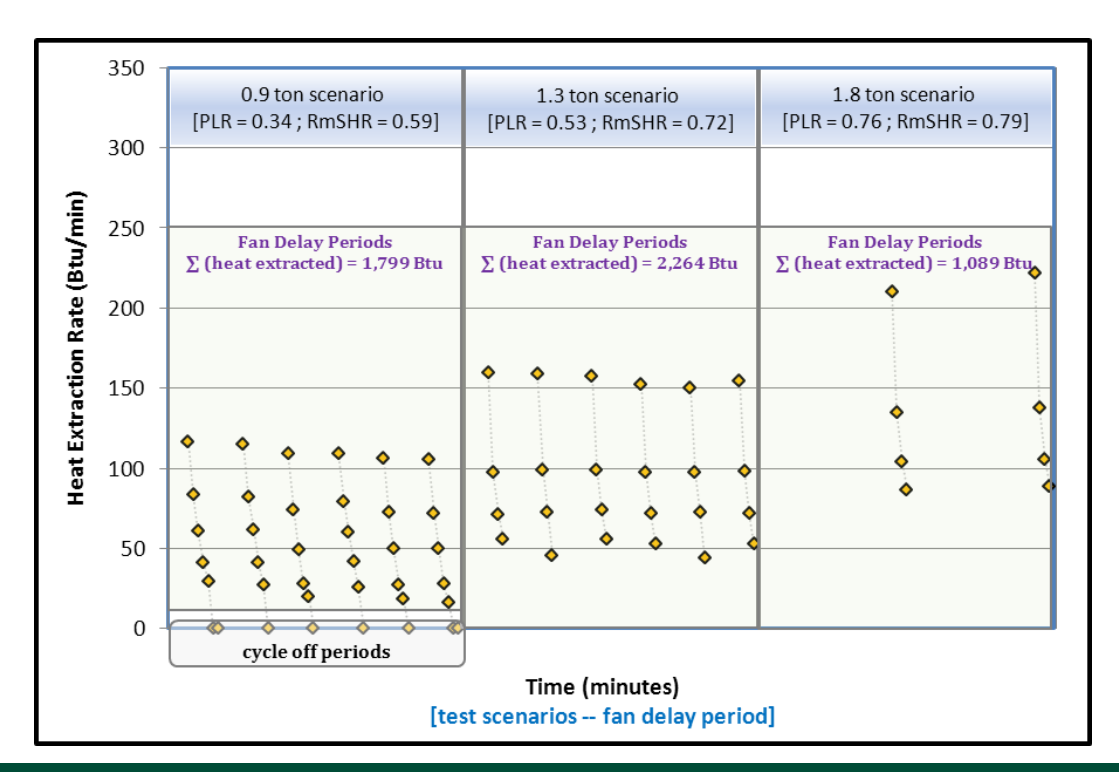


FIGURE 10. ONE-MINUTE PROFILE OF HEAT EXTRACTION RATE DURING FAN DELAY PERIOD [AIR-ENTHALPY METHOD]

NET ENERGY BENEFIT DURING FAN DELAY PERIOD

Table 2 summarizes the net energy benefit attained during the cumulated fan delay time of each one-hour test period. For the 0.9-ton scenario, net energy benefit during 30 minutes of fan delay time was 0.28 kilowatt hours (kWh). For the 1.3-ton scenario, net energy benefit during 24 minutes of fan delay time was 0.33 kWh. For the 1.8-ton scenario, net energy benefit during 8 minutes of fan delay time was 0.14 kWh. In spite of attaining similar equivalent cooling energy values for 0.9- and 1.3-ton scenarios, realized net energy benefits for the 1.3-ton scenario was higher than that for the 0.9-ton scenario. This was attributed to shorter fan delay time, hence less fan energy. Appendix D discusses the conceptual aspect of net energy benefit.

TABLE 2. SUMMARY OF NET ENERGY BENEFITS (DURING ONE-HOUR TEST PERIODS ONLY)

TEST SCENARIOS	AVERAGE NET SENSIBLE EER—DURING COOLING PERIODS (BTU/HR/W) [A]	TOTAL HEAT EXTRACTED— DURING FAN DELAY PERIODS (BTU) [B]	EQUIVALENT COOLING ENERGY (KWH) {(B÷A)÷ (1,000W)}	TOTAL FAN ENERGY— DURING FAN DELAY PERIODS (KWH) [D]	NET ENERGY BENEFIT— DURING FAN DELAY PERIODS (KWH) {C - D} [E]
0.9-Ton Scenario	3.68	1,799	0.49	0.21	0.28
1.3-Ton Scenario	4.51	2,264	0.50	0.17	0.33
1.8 Ton Scenario	5.38	1,089	0.20	0.06	0.14

ENERGY SAVINGS POTENTIAL

Table 3 presents the energy savings potential. The energy savings potential signifies the proportion of realized net energy benefit during fan delay periods relative to total system energy usage during cooling periods.

Figure 11 plots the energy savings potential against the PLRs. As the PLRs increased from 0.34 to 0.76, the potential for energy savings reduced from 20.6% to 4.5%. This was expected because increased PLR was directly associated with increased compressor run times or cooling periods. Thus, at higher PLRs, energy savings opportunities diminished due to the increase in run time of the A/C unit.

-	'ADIE 2	CHAMADY OF ENERGY	CAVINGO DOTENTIAL /D	URING ONE-HOUR TEST PERIODS ONLY)
	ABLE J.	JUNINARY OF ENERGY	SAVINGS FUIENTIAL ID	JURING ONE-HOUR TEST PERIODS ONLY)

TEST SCENARIOS	NET ENERGY BENEFIT (KWH)—DURING FAN DELAY PERIODS [E]	Total System Energy (kWH)—During Cooling Periods [F]	PERCENTAGE OF ENERGY SAVINGS POTENTIAL (UNCERTAINTIES) [E ÷ F]
0.9 -Ton Scenario	0.28	1.35	20.6% (± 20.4%)
1.3-Ton Scenario	0.33	2.27	14.6% (± 14.9%)
1.8-Ton Scenario	0.14	3.19	4.5% (± 12.1%)

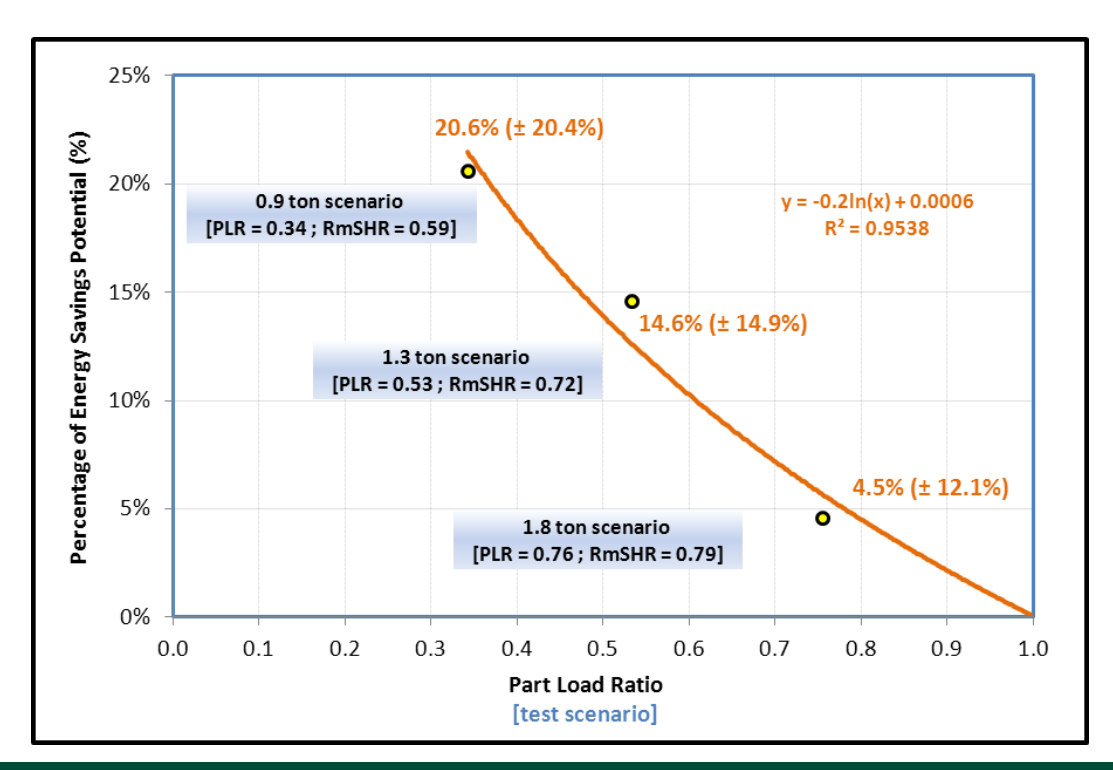


FIGURE 11. ENERGY SAVINGS POTENTIAL AS A FUNCTION OF PART LOAD RATIOS

ESTIMATING ANNUAL ENERGY SAVINGS

The energy savings potential as a function of PLRs shown in Figure 11 in conjunction with the A/C unit energy usage at different PLRs can be used to estimate the annual energy savings. The A/C unit energy consumption at various PLRs for a given CZ can be found by performing building energy simulation modeling.

To illustrate the methodology, building energy simulation modeling was performed. The input model for the energy simulation program (eQUEST, version 3-64) was an actual two story residential building. The input model was used to carry out energy simulation for all 16 CZs. Below lists the general features of the building.

Total building area: 2,227 sq ft Conditioned area: 1,768 sq ft

Floor: slab on grade

Exterior wall: wood frame, stucco, dry wall with batt R-19

Roof: concrete tile with ceiling insulation of batt R-38

Windows: vinyl double pane low-e with shading coefficient of 0.26

A/C unit: 3.5-ton split with seasonal energy efficiency ratio of 13

The eQUEST simulation platform was programmed to report the hourly data on four key variables. These variables were the cooling load of the building, cooling capacity of the A/C unit, condensing unit energy, and the indoor fan energy. The cooling load and capacity were used to determine the hourly PLRs and accordingly the percentage of energy savings using test data in Figure 11. The energy usage of the A/C unit at every PLR was determined by adding the energy usage of the condensing unit and indoor fan. The product of the percentage of energy savings and energy usage of the

A/C unit was totalized to provide the annual energy savings. Table 4 summarizes the results for all 16 CZs. The spreadsheet in Appendix E details all the hourly simulation results and energy saving values for all 16 CZs.

Table 4. Annual Cooling Energy Savings in all 16 Climate Zones – Single Family Residence

CLIMATE ZONE	ANNUAL A/C RUN TIME (HOURS/YR)— FROM SIMULATION	ANNUAL A/C ENERGY USAGE (KWH/YR)—FROM SIMULATION [G]	ANNUAL A/C ENERGY SAVINGS (KWH/YR) [H]	PERCENTAGE OF ANNUAL COOLING ENERGY SAVINGS [H÷G]
1	239	100	28	28%
2	1,716	2,052	324	16%
3	1,120	742	184	25%
4	1,719	1,835	331	18%
5	1,241	1,157	236	20%
6*	1,647	1,199	293	24%
7	1,783	1,540	323	21%
8*	2,275	2,526	425	17%
9*	2,399	2,964	454	15%
10*	2,705	3,599	490	14%
11	2,241	3,363	383	11%
12	1,974	2,804	373	13%
13*	2,966	4,762	501	11%
14*	2,794	4,264	431	10%
15*	5,141	9,021	814	9%
16*	1,083	1,181	187	16%

^{*} Climate Zones within SCE's Service Territory

CONCLUSIONS

This assessment involved conducting ten test scenarios comprised of various fan delay periods under three part load conditions. After a close review of test findings, only three test scenarios proved to be the most beneficial. These were test scenarios with four to five minutes of fan delay periods under every single part load condition.

Delaying the evaporator fan cycle off time had no impact on the overall power demand of the tested single-speed A/C unit. A/C units with single-speed compressor typically operate at full capacity even during periods when cooling load in the conditioned space is less than the A/C unit's cooling capacity. Under such conditions, while the compressor may operate at full load without substantial variations in power demand, its run time will decrease. For optimum delay times of four to five minutes, as the PLR increased from 0.34 to 0.76, the energy savings reduced from 20.6% to 4.5%. As the PLR approached unity (1.0 or 100%), the energy savings diminished. Clearly, energy savings varied as a function of PLRs.

RECOMMENDATIONS

Results indicated the fan delay technology to be more beneficial for climates where the A/C is expected to operate largely under low PLRs. To establish the annual energy savings for various building characteristics such as vintages and sizes, it is recommended to repeat the methodology described in "Estimating Annual Energy Savings" section.

APPENDIX A - INSTRUMENTATION

Table 5 provides the specifications and calibration dates for all sensors used in this project. Calibration of all instruments occurred prior to conducting any tests.

Table 5. Specifications, Calibration Dates, Locations, and Corresponding Monitoring Points for Sensors				
SENSOR TYPE	Make/Model	ACCURACY (NIST TRACEABLE)	Calibration Date (location)	Corresponding Key Monitoring Points
Temperature (type-T thermocouples)	Masy Systems, Ultra-Premium Probe	± 0.18°C [at 0°C] (± 0.32°F)	5-4-2011 (In-house)	 Inlet of evap fan Inlet of evap Outlet of evap Indoor room Outdoor room All refrigerant temps
Relative Humidity (RH)	Vaisala, HMP 233	± 1% (0-90% RH) ± 2% (90-100% RH)	5-5-2011 (SCE's Metrology Lab)	Outlet of evap
Wet Bulb	Vaisala, HMP 247	± 0.013% of reading	5-9-2011 (SCE's Metrology Lab)	• Indoor room
Relative Humidity (RH)	Vaisala, HMP 247	± (0.5 + 2.5% of reading)% RH	5-9-2011 (SCE's Metrology Lab)	Indoor room
Dew Point	Edgetech, Dew Prime DF Dew Point Hygrometer	± 0.2°C (± 0.36°F)	5-5-2011 (SCE's Metrology Lab)	 Inlet of evap Outlet of evap
Pressure (0-1000 psi)	Setra, C207	± 0.13% of full scale	4-14-2011 (In-house)	DischargeInlet TXV
Pressure (0-500 psi)	Setra, C207	± 0.13% of full scale	4-14-2011 (In-house)	SuctionOutlet evap
Pressure (0-10 inches of water, inwg)	Ashcroft, AQS- 28304	± 0.06% of full scale	4-14-2011 (Tektronix Calibration Lab)	Across indoor unit
Power	Ohio Semitronics, GW5-002C	± 0.2% of reading ± 0.04% of full scale (cond: 1,000W FS) (comp: 5,000W FS)	5-11-2011 (In-house)	Condensing unitCompressorCondenser fan
Power	HIOKI 3169-21	± 0.5% of reading	5-10-11 (In-house)	 Indoor unit Evap fan
Refrigerant Mass Flow Meter	Endress-Hauser, (Corriolis meter) 80F08- AFTSAAACB4AA	For liquids, ± 0.15% of reading For gases, ± 0.35% of reading	7-22-2010 (Homer R. Dulin Co.)	Refrigerant flow rate
Scale	HP-30K	± 0.1 gram (± 0.0035 ounces)	11-29-2010 (In-house)	Mass of condensate

APPENDIX B - ENGINEERING CALCULATIONS

Using air and refrigerant data, a series of calculations were performed to obtain the key performance parameters. The collected raw data was downloaded from the data acquisition system and reduced for next step calculations. $\mathsf{XProps^{TM}}$ refrigerant property program, version 1.5, was used to analyze refrigerant properties. The thermodynamic properties of air, specifically enthalpies, were determined according to the 2005 ASHRAE Handbook of Fundamentals.³

GROSS AND NET COOLING CAPACITY

The gross cooling capacity is the rate of cooling or heat removal (Btu/hr) that takes place at the evaporator coil of the unit. Cooling capacity was determined based on two methods, air-enthalpy and refrigerant-enthalpy methods. In the air-enthalpy method, cooling capacity was determined based on the properties of air entering and leaving the indoor unit, and the associated airflow rate (Equation 1).

EQUATION 1. GROSS COOLING CAPACITY (AIR-ENTHALPY METHOD)

$$\overset{\text{g}}{Q}_{\text{gross-air}} = \text{cfm}' \text{ r}' \left(h_{\text{inlet-air}} - h_{\text{outlet-air}} \right)' \text{ CFT}$$

where,

 $\overset{\mathring{\text{e}}}{Q}_{\text{gross- air}}$ = gross cooling capacity of air, Btu/hr

cfm = volumetric airflow rate, ft³/min

 ρ = density of air, lb/ft³

 $h_{inlet-air}$ = enthalpy of air entering the evaporator coil, Btu/lb

 $h_{autlet. air}$ = enthalpy of air leaving the evaporator coil, Btu/lb

CFT = conversion factor for time, 60 min/hr

The cooling capacity in the refrigerant-enthalpy method was based on the mass flow rate of refrigerant, as well as the refrigerant enthalpies at the inlet and outlet of the evaporator coil (Equation 2). The difference between refrigerant enthalpies at inlet and outlet of the evaporator coil are referred to as the refrigeration effect. It is the quantity of heat that each unit mass of refrigerant absorbs to cool the refrigerated space. It simply represents the capacity of the evaporator per pound of refrigerant.

EQUATION 2. GROSS COOLING CAPACITY (REFRIGERANT-ENTHALPY METHOD)

$$\overset{g}{Q}_{aross-refrig} = \overset{g}{m}_{refrig} \cdot (h_{inlet-refrig} - h_{outlet-refrig})$$

Where,

 ${Q}_{aross-refrig}$ = gross cooling capacity of refrigerant, Btu/hr

 m_{refrig} = refrigerant mass flow rate, lb/hr

 $h_{inlet-refrig}$ = sub-cooled liquid refrigerant enthalpy at expansion valve

inlet, (Btu/lb)

 $h_{\text{outlet-refrig}}$ = superheated refrigerant enthalpy at the evaporator exit,

(Btu/lb)

To exclude the heat input of the evaporator fan motor from total cooling capacity, net cooling capacity was calculated. The net cooling capacity was determined by simply subtracting the heat gain due to evaporator fan motor from the gross cooling capacity obtained by the air-enthalpy method (Equation 3).

EQUATION 3. NET COOLING CAPACITY (AIR-ENTHALPY METHOD)

$$\overset{\text{g}}{Q}_{\text{net- air}} = \overset{\text{g}}{Q}_{\text{gross- air}}$$
 - $\left(kW_{\text{evap- fan}} \text{ ' CFP}\right)$

Where,

 $\dot{\tilde{Q}}_{\text{net-air}}$ = net cooling capacity of air, Btu/hr

 $\overset{\text{g}}{Q}_{\text{aross-air}}$ = gross cooling capacity of air, Btu/hr

kW_{evan, fan} = evaporator fan motor power, kW

CFP = conversion factor for power, 3,413 Btu/hr/kW

GROSS AND NET SENSIBLE COOLING CAPACITY

Using air properties at the inlet and outlet of the indoor unit, total or gross sensible cooling capacity of the evaporator coil was obtained (Equation 4). To account for the evaporator fan motor heat, the net sensible cooling capacity was calculated as well (Equation 5).

EQUATION 4. GROSS SENSIBLE COOLING CAPACITY (AIR-ENTHALPY METHOD)

$$\overset{g}{Q}_{qross-\ sensible} = cfm'\ r'\ C_{n}'\ (T_{inlet.\ air}\ -\ T_{outlet.\ air})'\ CFT$$

Where,

 $\mathring{\mathring{Q}}_{aross-sensible}^{g}$ = gross sensible cooling capacity of air, Btu/hr

cfm = volumetric airflow rate, ft³/min

 ρ = density of air, lb/ft³

C_o = specific heat of air, Btu/Ib-°F

 $T_{inlet-air}$ = entering air temperature, °F

 $T_{outlet-air}$ = leaving air temperature, °F

CFT = conversion factor for time, 60 min/hr

EQUATION 5. NET SENSIBLE COOLING CAPACITY (AIR-ENTHALPY METHOD)

$$\overset{\text{g}}{\check{Q}}_{\text{net- sensible}} = \overset{\text{g}}{\check{Q}}_{\text{gross- sensible}} \text{ - } \left(kW_{\text{evap- fan}} \text{ ' CFP}\right)$$

Where,

 $\overset{\text{g}}{Q}_{\text{net-sensible}}$ = net sensible cooling capacity of air, Btu/hr

 $\overset{g}{Q}_{aross-sensible}$ = gross sensible cooling capacity of air, Btu/hr

 $kW_{evap-fan}$ = evaporator fan motor power, kW

CFP = conversion factor for power, 3,413 Btu/hr/kW

EVAPORATOR COIL SENSIBLE HEAT RATIO (SHR)

The sensible heat ratio (SHR) of evaporator coil was determined using Equation 6. It compares the amount and proportion of sensible cooling to the total cooling capacity.

EQUATION 6. SENSIBLE HEAT RATIO (AIR-ENTHALPY METHOD)

$$SHR = \frac{\overset{g}{Q}_{gross-\; sensible}}{\overset{g}{Q}_{gross-\; air}}$$

Where,

SHR = sensible heat ratio, unit-less

 $\overset{{}_{g}}{Q}_{gross- \, sensible}$ = gross sensible cooling capacity of air, Btu/hr

 \mathring{Q}_{gross} = gross cooling capacity of air, Btu/hr

PART LOAD RATIO (PLR)

The part load ratio (PLR) is the ratio of total cooling load to the total cooling capacity of the unit (Equation 7). In this case, the total cooling load is the imposed cooling load in the indoor test chamber. The manufacturer, however, publishes the total capacity of the unit. The manufacturer's list the unit cooling capacities as a function of outdoor and indoor conditions.

EQUATION 7. PART LOAD RATIO

$$PLR = \frac{\overset{g}{Q}_{\text{total- cooling- load}}}{\overset{g}{Q}_{\text{total- capacity}}}$$

Where,

PLR = part load ratio, unit-less

 $\overset{\circ}{Q}_{total-cooling-load}$ = imposed total cooling load in indoor test chamber, Btu/hr

 $\overset{g}{Q}_{\text{total- capacity}}$ = total cooling capacity of the unit at the operating conditions, Btu/hr

ENERGY EFFICIENCY RATIOS (EERS)

The energy efficiency ratio (EER) of the unit depends on the total power input, as well as the cooling capacity of the unit. The total power input includes compressor, condenser fan, and evaporator fan. The net EER of the unit was determined by dividing the net cooling capacity of air by the measured total input power to the unit (Equation 8). The net sensible EER of the unit was determined by dividing the net sensible cooling capacity of air by the measured total input power input to the unit (Equation 9).

EQUATION 8. NET ENERGY EFFICIENCY RATIO (AIR-ENTHALPY METHOD)

$$\mathsf{EER}_{\mathsf{NET}} = \frac{\overset{\mathtt{g}}{\mathsf{Q}}_{\mathsf{net-\; air}}}{\mathsf{W}_{\mathsf{total}}}$$

Where,

 EER_{NET} = net energy efficiency ratio of the unit, Btu/hr/W

 $\overset{\text{g}}{Q}_{\text{net-air}}$ = net cooling capacity of air, Btu/hr

 W_{total} = measured total input power to the A/C unit, W

EQUATION 9. NET SENSIBLE ENERGY EFFICIENCY RATIO (AIR-ENTHALPY METHOD)

$$EER_{\text{NET- Sensible}} = \frac{\overset{\text{g}}{Q}_{\text{net- sensible}}}{W_{\text{total}}}$$

Where,

 $EER_{NFT. Sensible}$ = net sensible energy efficiency ratio of the unit, Btu/hr/W

 $\overset{g}{Q}_{net, sensible}$ = net sensible cooling capacity of air, Btu/hr

 W_{total} = measured total input power to the A/C unit, W

EVAPORATOR COIL SUPERHEAT AND CONDENSER COIL SUB-COOLING

One of the system parameters is the evaporator coil superheat. The evaporator coil superheat was determined based on the vapor refrigerant temperature at the outlet of the evaporator coil and the saturation temperature of refrigerant corresponding to the pressure at the evaporator outlet (Equation 10).

EQUATION 10. EVAPORATOR COIL SUPERHEAT

 $SH_{evap} = T_v - SET$

Where,

 SH_{evap} = evaporator coil superheat, °F

 T_v = vapor refrigerant temperature at the outlet of the evaporator

coil, °F

SET = saturated evaporating temperature based on evaporator

outlet pressure, °F

Equation 11 was used to determine the condenser sub-cooling. Condenser sub-cooling was obtained by subtracting the liquid refrigerant temperature at the outlet of the condenser from the saturated condensing temperature based on compressor outlet pressure.

EQUATION 11. CONDENSER COIL SUB-COOLING

$$SC_{cond} = SCT - T_{L}$$

Where,

 SC_{cond} = condenser coil sub-cooling, °F

SCT = saturated condensing temperature based on condenser outlet

pressure, °F

 T_1 = liquid refrigerant temperature at the outlet of the condenser

coil, °F

POWER AND ENERGY

The power usage associated with the A/C components was read directly from the data acquisition system. These measurements included the indoor and outdoor units' power. The indoor unit power was comprised of the evaporator fan motor and circuit board electronics. The outdoor units' power included compressor and condenser fan motor. Equation 12 was used to obtain the total system power of the A/C unit.

EQUATION 12. TOTAL AIR-CONDITIONING UNIT POWER

 $kW_{Total} = kW_{evap\text{-}fan} + kW_{electronics} + kW_{compressor} + kW_{cond\text{-}fan}$ Where,

 kW_{Total} = power usage by the A/C unit, kW

 $kW_{evap-fan}$ = power usage by the evaporator fan motor, kW

 $kW_{electronics}$ = power usage by the indoor unit circuit board electronics, kW

 $kW_{compressor}$ = power usage by the compressor, kW

 $kW_{cond-fan}$ = power usage by the condenser fan motor, kW

The energy consumption is defined as the product of supplied power and total hours of power usage. Equation 13 shows the general format for obtaining energy usage. After determining the energy usage of each component, the total energy usage was obtained by adding all the individual components together. Therefore, the total energy usage included evaporator fan motor, circuit board electronics, compressor, and condenser fan motor.

EQUATION 13. ENERGY USAGE

 $kWh = kW \times t$

Where,

kWh = energy usage by end-use, kWh

kW = average power usage by end-use, kW
t = time of power usage by end-use, hours

APPENDIX C - MEASUREMENT UNCERTAINTY

The carried out uncertainty analysis followed guidelines provided by the national and international standards.⁴ The following list summarizes the general steps and procedures used to evaluate uncertainties.

- 1. Quantify the components of standard uncertainties for a single measurement
- 2. Calculate the combined uncertainty
- 3. Calculate the expanded uncertainty

QUANTIFY COMPONENTS OF STANDARD UNCERTAINTIES FOR A SINGLE MEASUREMENT

For a single measurement in this project, two sources or components of uncertainties were identified. Each source was estimated using an appropriate method. One source of uncertainty was the accuracy of the measuring instrument, or sensor, specified by the manufacturer. This was obtained using a non-statistical evaluation method. The other source was the repeated measurements, which required using statistical means to evaluate. Both methods were used to determine the magnitude and associated uncertainty for a single measured quantity.

The manufacturers of the measuring instruments either reported the sensor accuracy as an upper and lower limit, or based on the readings. If lower and upper limits were provided, a rectangular or uniform distribution was used (Equation 14). If accuracies were based on the readings, a triangular distribution was used. The assumption was that the values close to the measurement (center) were more likely than the values close to the limits or extremes (Equation 14).

EQUATION 14. STANDARD UNCERTAINTY WITH SENSOR SPECIFICATIONS (RECTANGULAR AND TRIANGULAR DISTRIBUTIONS)

$$u(x_i) = \frac{|a|}{\sqrt{3}}$$
 (Rectangular distribution) $u(x_i) = \frac{|a|}{\sqrt{6}}$ (Triangular

distribution)

Where,

 $u(x_i)$ = standard uncertainty associated with sensor specification

a = absolute value of upper and lower limits

For repeated measurements, the standard uncertainty was the same as the standard deviation of the mean. Subsequently, it involved determining the arithmetic mean of measurements, standard deviation of measurements, and standard deviation of the arithmetic mean of measurements. Equation 15 illustrates the standard uncertainty for repeated measurements, and in this case standard deviation of the mean.

EQUATION 15. STANDARD UNCERTAINTY FOR REPEATED MEASUREMENTS (STANDARD DEVIATION OF MEAN)

$$u(x_j) = s(\bar{x}) = \frac{s(x_j)}{\sqrt{n}} = \sqrt{\frac{\sum_{j=1}^{n} (x_j - \bar{x})^2}{n (n-1)}}$$

Where,

 $u(x_i)$ = standard uncertainty for repeated measurements

 $s(\bar{x}) = \text{standard deviation of sample mean}$

 $s(x_i) = standard deviation of samples$

n = number of samples

 x_i = sampled values

 \bar{x} = sample mean

After determining the sources of uncertainties for a single measurement or quantity, they were combined to a single standard uncertainty value for that quantity. Subsequent sections cover this topic.

CALCULATE THE COMBINED UNCERTAINTY

The notion of combining uncertainties follows the law of propagation of uncertainties. This is analogous to the law of propagation of errors. It combines the contributions from each component or source of uncertainty to the results. For single quantities or measurements like temperature and pressure, the contribution of sensor accuracy and measurement repeatability were combined to provide the overall standard uncertainty for that quantity or measurement. Equation 16 illustrates this measurement.

EQUATION 16. COMBINED STANDARD UNCERTAINTY FOR A SINGLE MEASUREMENT

$$u(x_{c}) = \sqrt{\frac{\hat{g}_{1}(x_{i})\hat{y}_{1}^{2} + \hat{g}_{1}(x_{j})\hat{y}_{1}^{2}}{}}$$

Where,

 $u(x_c)$ = combined standard uncertainty for a single measurement

 $u(x_i)$ = standard uncertainty associated with sensor specifications

 $u(x_i)$ = standard uncertainty of repeated measurements

These single measurements were used in equations to obtain other desired and key parameters. For example, gross cooling capacity using refrigerant-enthalpy method was a function of refrigerant mass flow rate and enthalpies at the inlet and outlet of evaporator coil. Therefore, to estimate the standard uncertainty for calculated gross cooling capacity values, the standard uncertainties associated with refrigerant mass flow rate and enthalpies were used.

Equation 17 shows the general format for combining standard uncertainties for non-correlated input quantities. Non-correlated input quantities means the uncertainties of input quantities are independent. The sensitivity coefficient in Equation 17 denotes mathematically how much "f" changes given an infinitesimal change in " x_i ". It is a conversion factor for converting the units of an input quantity into the units of measurement. Since the units of input quantities were the same as the measurements, the sensitivity coefficient was not a concern for this project.

EQUATION 17. GENERAL EQUATION FOR COMBINING STANDARD UNCERTAINTIES [NON-CORRELATED QUANTITIES]

$$u_{c}(y) = \sqrt{\underset{n=1}{\overset{n}{\underset{g}{\overset{e}{\underbrace{\P f} \frac{O}{\underbrace{O}}}{\underbrace{D}}}}} u^{2}(x_{i})}$$

Where,

 $u_c(y)$ = combined standard uncertainty

 $\frac{\P f}{\P x_i} = c_i \qquad = \text{sensitivity coefficient}$

 $u(x_i)$ = standard uncertainty

Equation 17 becomes much simpler for relationships involving sums and products. Equation 18 demonstrates relationships involving sums or differences. Equation 19 shows relationships involving products or quotients. In Equation 19, both relative and absolute forms display.

EQUATION 18. COMBINED STANDARD UNCERTAINTY FOR EQUATIONS INVOLVING SUMS OR DIFFERENCES

$$u_{c}(y) = \sqrt{\frac{4}{6}u(x_{c})_{1}^{2}u^{2} + \frac{4}{6}u(x_{c})_{2}^{2}u^{2} + L + \frac{4}{6}u(x_{c})_{1}^{2}u^{2}}$$

Where,

 $u_c(y)$ = combined standard uncertainty for calculated parameter of interest

 $U(x_c)_{1,2,K,n}$ = standard uncertainty from each contributor or input quantity

EQUATION 19. COMBINED STANDARD UNCERTAINTY FOR EQUATIONS INVOLVING PRODUCTS OR QUOTIENTS

$$\frac{u_{c}(y)}{|y|} = \sqrt{\frac{\frac{au}{b}(x_{c})_{1}\frac{\dot{o}^{2}}{\dot{c}}}{k_{1}} + \frac{au}{b}(x_{c})_{2}\frac{\dot{o}^{2}}{\dot{c}}} + L + \frac{au}{b}(x_{c})_{n}\frac{\dot{o}^{2}}{\dot{c}}}{k_{2}}}$$
 (Relative form)

$$u_c(y) = \left| y \right| \sqrt{\frac{gu(x_c)_1 \frac{\ddot{o}^2}{\dot{\pm}}}{x_1 \frac{\ddot{c}}{\dot{\pm}}} + \underbrace{\frac{gu(x_c)_2 \frac{\ddot{o}^2}{\dot{\pm}}}{x_2 \frac{\ddot{c}}{\dot{\pm}}} + L + \underbrace{\frac{gu(x_c)_n \frac{\ddot{o}^2}{\dot{\pm}}}{x_n \frac{\ddot{c}}{\dot{\pm}}}}_{\text{(Absolute form)}}$$

Where,

 $u_c(y)$ = combined standard uncertainty for calculated parameter of interest

y = absolute value of calculated parameter of interest

 $U(x_c)_{1,2,K,n}$ = standard uncertainty from each contributor or input quantity

 $X_{1,2K,n}$ = measured values for each input quantity

CALCULATE THE EXPANDED UNCERTAINTY

It is important to note that the resulting combined standard uncertainties discussed above are based on a 68% confidence level. Although it is beyond the scope of this report to show this fact, it suffices to say that the combined standard uncertainties take the form of a normal distribution in accordance with the central limit theorem. Consequently, as the input uncertainties are combined and expressed in terms of a standard uncertainty, the resulting normal distribution is expressed as one standard deviation. One standard deviation covers about 68% of the area under the normal distribution curve. When using standard uncertainties for reporting uncertainty limits, there is about 68% confidence that the measured or calculated parameter of interest lies within the stated limits.

Thus, to boost confidence levels, it is a generally accepted practice to expand the standard uncertainties from one standard deviation to two standard deviations, or 95% confidence level. This can be done by simply multiplying the combined standard uncertainty by a coverage factor of 2, or using critical values for normal distribution (Equation 20). In this project, the critical values for t-distribution at 95% confidence

level were used. These values were obtained using "n-1" degrees of freedom with "n" being the number of samples.

EQUATION 20. EXPANDED STANDARD UNCERTAINTY

$$U_{expanded}(y) = u_c(y)' t_{a,u}$$

Where,

 $U_{\text{expanded}}(y)$ = expanded standard uncertainty for calculated parameter of interest

 $u_c(y)$ = combined standard uncertainty for calculated parameter of interest

 $t_{\rm a,u}$ = critical values for t-distribution at 95% confidence level (α

= 0.05, two-tailed curve) corresponding to appropriate degrees of freedom ($\nu = n-1$)

APPENDIX D – TEST SCENARIOS AND PRELIMINARY RESULTS

TEST SCENARIOS

In total, 10 test scenarios were conducted (Table 6). The duration of every test was one hour. For every test, the thermostat was set to $75^{\circ}F$ with a cut-in and cut-off point of \pm 0.7°F. The outdoor test chamber maintained a DBT at 115°F. Cooling load in the indoor test chamber was set to 0.9, 1.3, and 1.8 tons. The indoor test chamber (room) sensible heat ratios (RmSHRs) were 0.59, 0.72, and 0.79 (Table 6). RmSHRs indicate the ratio of sensible to total cooling load.

For every test, portable heaters were used to impose and keep a constant sensible load on the A/C unit during the entire test period. Input power of portable heaters was set to 1.85 kilowatt (kW) for 0.9-ton test runs, 3.28 kW for 1.3-ton test runs, and 5.00 kW for 1.8-ton runs. Ultrasonic humidifiers were used to impose constant latent load on the A/C unit. For all test runs, humidifiers introduced 4 pounds-perhour (lbs/hr) of moisture into the indoor test chamber. Essentially, for all test runs the latent load stayed fixed while the sensible load varied. This allowed capturing performance differences as a function of sensible load variations. As data gathering continued, observations revealed that for the 1.3-ton test runs the A/C compressor off time did not exceed 4 minutes. So, for the 1.8-ton scenarios 5- and 10-minute delay periods were excluded.

TABLE 6. SUMMARY OF ALL TEST SCENARIOS						
TEST SCENARIOS	IMPOSED INTERNAL SENSIBLE LOAD (BTU/HR & TON)	IMPOSED INTERNAL LATENT LOAD (BTU/HR & TON)	TOTAL IMPOSED INTERNAL LOAD (BTU/HR & TON)	ROOM SENSIBLE HEAT RATIO (RMSHR) FOR IMPOSED LOAD	OUTDOOR AMBIENT TEMPERATURE (°F)	FAN DELAY TIME (MINUTES)
1						2
2	6,314	4,452	10,766		115	5
3	Btu/hr	Btu/hr	Btu/hr	0.59		10
4	0.5 Ton	0.4 Ton	0.9 Ton			based on compressor run time
5						2
6	11,195	4,452	15,647		115	5
7	Btu/hr	Btu/hr	Btu/hr	0.72		10
8	0.9 Ton	0.4 Ton	1.3 Ton			based on compressor run time
9	17,065	4,452	21,517			2
10	Btu/hr 1.4 Ton	Btu/hr 0.4 Ton	Btu/hr 1.8 Ton	0.79	115	based on compressor run time

SELECTED TEST SCENARIOS FOR ANALYSIS

To focus attention on the project objectives, test runs with the highest benefits from each group (0.9, 1.3, and 1.8 ton) were selected for analysis. The benefits reflected the amount of sensible heat extracted from evaporator coil in the form of electrical energy relative to fan energy used to provide that amount of cooling during fan delay periods. This involved establishing the optimum period for delaying evaporator fan of the A/C unit under test. Looking at the complete set of test runs the same pattern, with optimal delay time between 4 and 5 minutes, was observed. As a result, test runs with four or five minutes of delay periods were considered for analysis.

Figure 12 illustrates the representative pattern observed for seven minutes of delay time interval. The horizontal straight line is the fan power. The negative sloped curve is the cooling power equal to sensible heat extracted from evaporator coil. The optimum fan delay period occurs when equivalent cooling power curve crosses the evaporator fan power input line. This is analogous to break-even point. As expected, the amount of sensible heat extracted and subsequently equivalent cooling power during the fan delay period decreased as a function of time. The triangular area under the curve to the left of the optimum point is the benefit region, and the triangular area to the right of the optimum point is the penalty region.

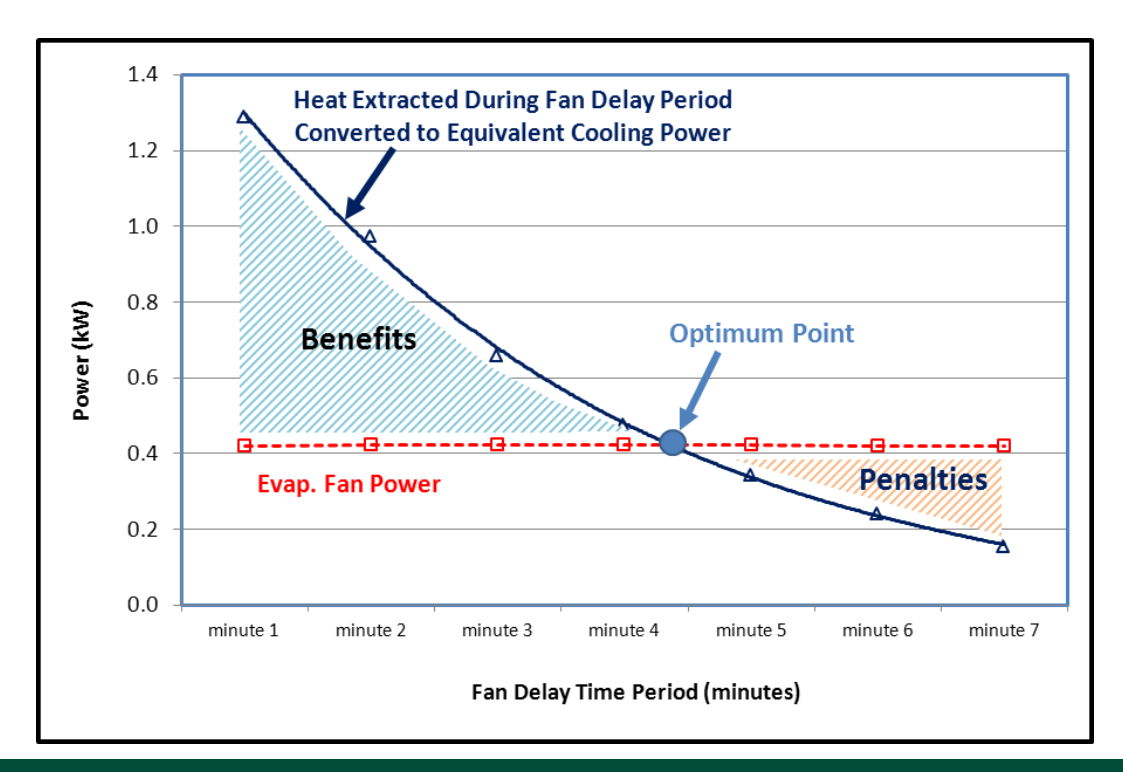


FIGURE 12. GRAPHICAL PRESENTATION OF AN OPTIMUM FAN DELAY PERIOD

One important remark with respect to Figure 12 is that the optimum point established here is specific to the A/C unit tested. Assuming heat extracted from the evaporator coil during delay periods remain unaffected, any change in fan power will alter the optimum point. For example, for bigger horsepower supply fans with higher power input, the fan power line in Figure 12 will shift upward. This upward shift will in turn move the optimum point to the left, indicating shorter than five-minute delay period as the optimum point. The opposite is true for smaller horsepower fans. Therefore, generalizing four to five minutes fan delay as the optimum point for all A/C units will be an incorrect conclusion drawn from Figure 12. This is particularly true for split A/C units because various combinations of indoor and outdoor units are available to choose from manufacturers. In addition, the selection of fan horsepower size is very much dependent on the duct length, hence static pressure drop.

Another criterion considered for selection was the uniformity and consistency of the delay periods within each cycle. Since observation showed that for some of the test runs the delay period occurred discretely over two cycles, it became important to examine the uniformity of delay cycles. For example, when the controller was set to delay the fan for 10 minutes under the 0.9-ton test scenario, the delay time was 8 minutes during the first cycle and 2 minutes during the subsequent cycle. In addition, when the controller was set to delay the fan for 5 minutes under 1.3-ton test scenario, the delay time was 3 minutes during the first cycle and 2 minutes during the subsequent cycle. To emphasize, this observation was true only for this controller. For proper operation, the controller should reset the timer for each cycle.

As a result, for 0.9-ton test scenario, the test run with a 5-minute delay period was selected to be included in the analysis. For the 1.3-ton test scenario, the test run with 4-minute delay periods was selected. Although for this particular test run the controller was set to delay the fan for 10 minutes, the system called for cooling after 4 minutes of delay time. Subsequently, the longest available delay time was 4

minutes for the 1.3-ton test scenario. For the 1.8-ton test scenario, the test run with a 4-minute delay time was also selected. For this test scenario, the longest available delay time was 4 minutes as well. To recap, tests 2, 7, and 10 listed in Table 6 were selected.

PART LOAD RATIOS CORRESPONDING TO TEST SCENARIOS

One of the key performance indicators of an A/C unit is the PLR. The PLR is the ratio of cooling load in the room to the manufacturer's rated cooling capacity of the A/C unit at a specified outdoor and indoor condition. Cooling load in the room reflects the imposed cooling load in the indoor environment test chamber. As listed in Table 7, for three test categories, the imposed latent load remained unchanged while the sensible portion varied. Accordingly, RmSHR was higher for 1.3- and 1.8-ton test scenarios.

TABLE 7. IMPOSED COOLING LOAD IN THE INDOOR TEST CHAMBER (ROOM) AND THE CORRESPONDING SENSIBLE HEAT RATIO							
IMPOSED COOLING LOAD AND CORRESPONDING SENSIBLE HEAT RATIO IN INDOOR TEST CHAMBER	0.9 Ton Scenario	1.3 Ton Scenario	1.8 Ton Scenario				
Imposed Latent Load in the Room, Btu/hr	4,452	4,452	4,452				
Imposed Sensible Load in the Room, Btu/hr	6,314	11,195	17,065				
Total Imposed Load in the room, Btu/hr	10,766	15,647	21,517				

0.72

Manufacturers publish total cooling capacity of the A/C unit as a function of outdoor DBT, and indoor DBT and WBT. In this project, all test scenarios were conducted at an outdoor DBT of 115°F and an indoor DBT of 75°F. Based on the measured indoor average WBT, cooling capacities were extracted from manufacturer's catalog (Table 8). The PLR for the 0.9-ton scenario turned out to be 0.34, for 1.3-ton scenario 0.53, and for 1.8-ton scenario 0.76.

0.59

0.79

Room Sensible Heat

Ratio (RmSHR)

TABLE 8. PART LOAD RA	TIO

Manufacturer's P Outdoor Dry-Bul 115°F and Ind Temperatu	B TEMPERATURE OF OOR DRY-BULB	TEST SCENARIOS [ALL AT INDOOR DRY-BULB TEMPERATURE OF 75°F]			
INDOOR WET-BULB TEMPERATURE (°F)	TOTAL CAPACITY (TON) [I]	AVERAGE ROOM WET- BULB TEMPERATURE (°F)	IMPOSED TOTAL COOLING LOAD (TON) [J]	PART LOAD RATIO (PLR) [J÷I]	
59	2.3				
61 [‡]	2.4	61	1.8	0.76	
63	2.4	63	1.3	0.53	
67	2.6	67	0.9	0.34	
71	2.8	l I			

 $^{^{\}scriptscriptstyle ext{t}}$ This point was obtained using linear interpolation since it was not published by the manufacturer.

INDOOR (ROOM) AND OUTDOOR (AMBIENT) CONDITIONS

Figure 13 depicts a one-minute DBT profile of indoor and outdoor test chamber over the entire one hour of test run for the selected three test scenarios. The average outdoor and indoor DBT for selected three test scenarios were maintained around 115° F and 75° F, respectively. In Figure 13, uncertainty values with average indoor and outdoor DBT measurements are followed by a \pm symbol. Appendix C covers procedures for evaluating measurement uncertainties.

Figure 14 presents the average WBT and RH attained in indoor test chamber over the entire one hour of test run for the selected three test scenarios. The uncertainties with average WBT and RH values are followed by a \pm symbol in Figure 14. As expected, drier indoor conditions were observed for test scenarios with higher RmSHR.

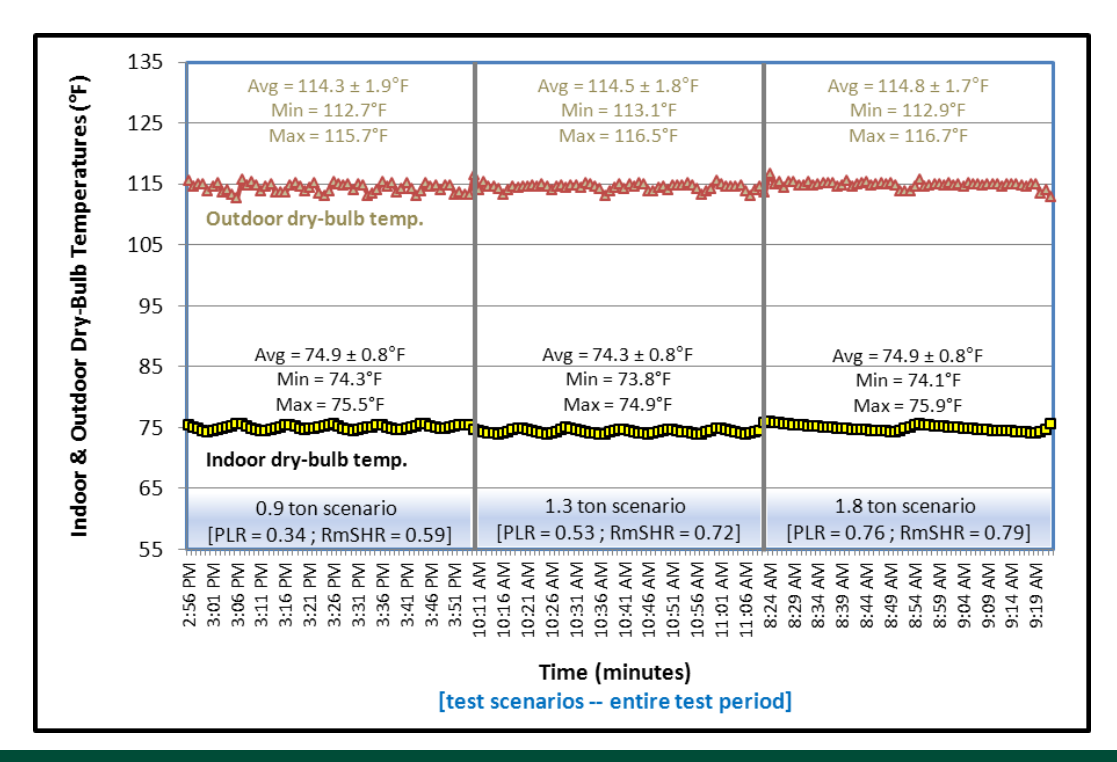


FIGURE 13. ONE-MINUTE PROFILE OF INDOOR (ROOM) AND OUTDOOR (AMBIENT) DRY-BULB TEMPERATURES

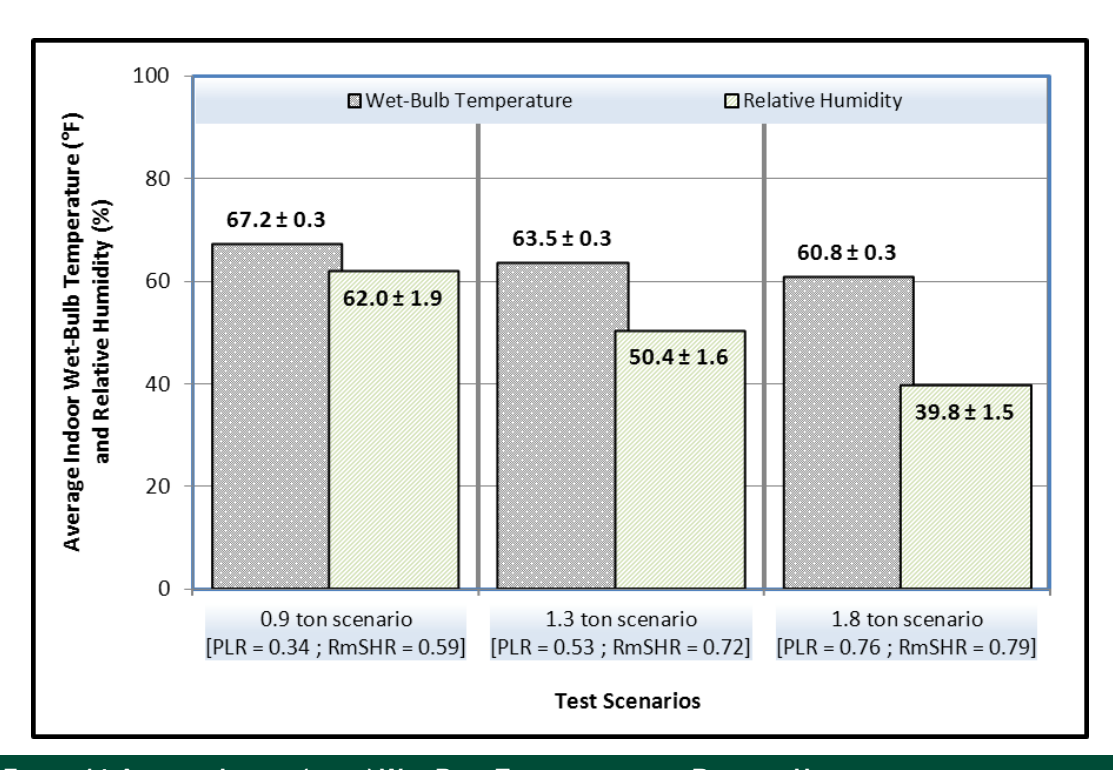


FIGURE 14. AVERAGE INDOOR (ROOM) WET-BULB TEMPERATURE AND RELATIVE HUMIDITY

Figure 15 exemplifies DBT variations in indoor test chamber during one complete cycle for 0.9-ton test scenario as a representative run. Here, a complete cycle refers to the period when the compressor first starts running until the next time it starts

again. Hence, a complete cycle included the cooling, fan delay, and cycle off periods, if any.

As shown in Figure 15, for this particular cycle the thermostat called for cooling when the indoor DBT was 75.4°F. This was the initiation of the cooling period, minute 1. As the compressor continued its normal operation, it pulled down the indoor DBT to 74.4°F, at minute 4. Therefore, within the first 4 minutes, the A/C unit pulled down the indoor DBT by 1.0°F. At this point, the thermostat setpoint was met and accordingly the compressor stopped running. This was the end of the cooling period and initiation of the fan delay period. On the other hand, the evaporator fan continued its operation until minute 9. During these 5-minutes of delay period, the indoor DBT went up by 0.5°F. The evaporator fan stopped running after the fan delay period ended. At this point, the entire unit cycled off, meaning both the compressor and evaporator fan cycled off. The cycle off period lasted for two minutes, minute 11. At the end of this cycle off period, when the indoor DBT reached 75.5°F, the thermostat called for cooling again and the next cycle started.

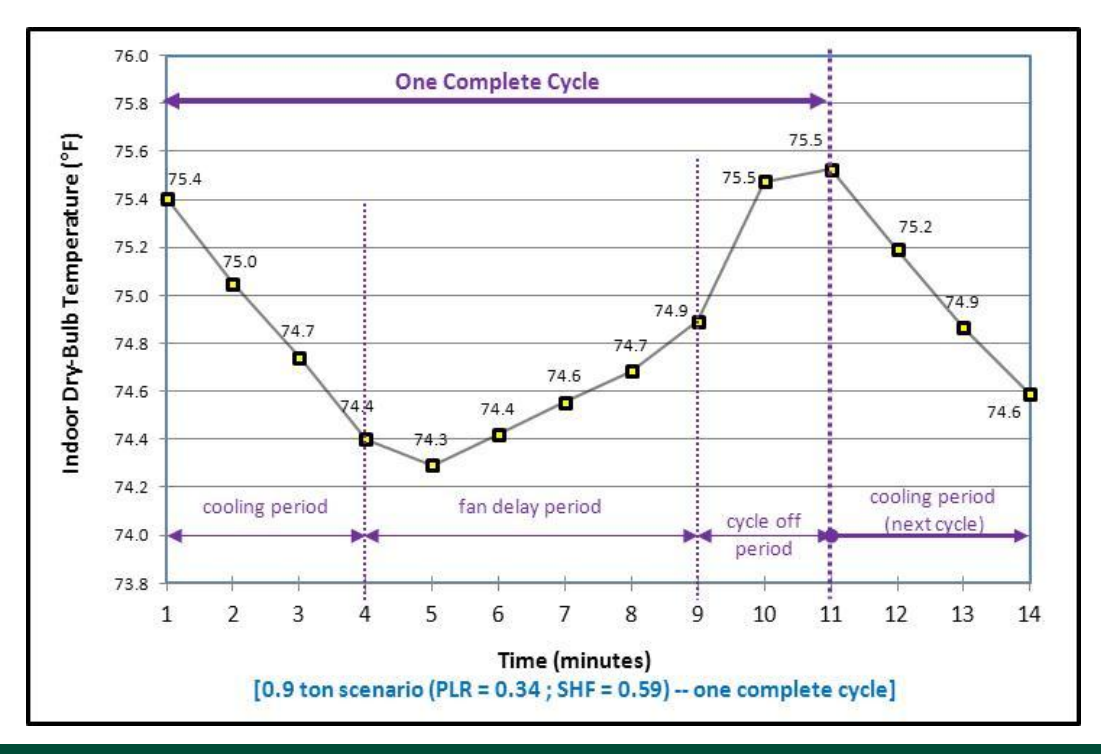


FIGURE 15. INDOOR (ROOM) DRY-BULB TEMPERATURE AND RELATIVE HUMIDITY DURING ONE COMPLETE CYCLE [0.9 TON TEST SCENARIO]

COMPARISON OF GROSS (TOTAL) COOLING RATE

To gain confidence in the cooling rate values, gross or total cooling rates using air-and refrigerant-enthalpy methods were compared for the selected three test scenarios (Figure 16). The difference between average gross cooling rate values using air- and refrigerant-enthalpy methods was within the industry recommended acceptable range of 6%, or less. In Figure 16 measurement uncertainties are shown after \pm symbol.

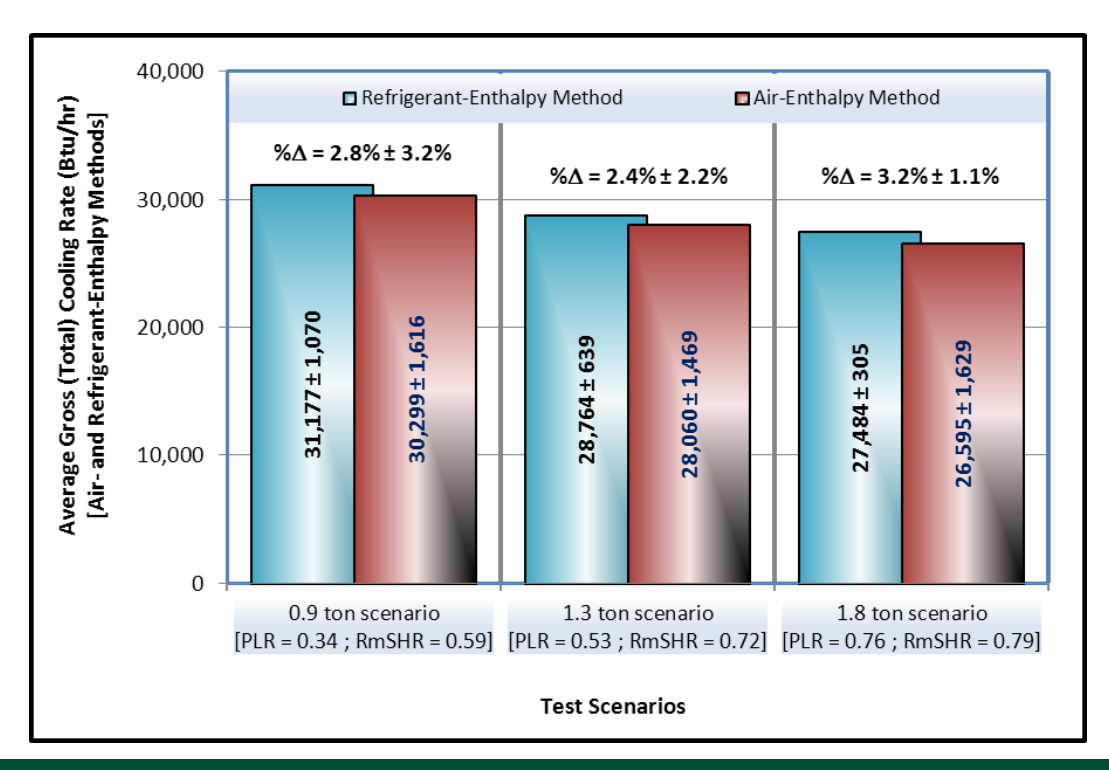


FIGURE 16. AVERAGE GROSS (TOTAL) COOLING RATE - AIR- AND REFRIGERANT-ENTHALPY METHODS

APPENDIX E - HOURLY SIMULATION REPORT

The following spreadsheet contains hourly simulation results for all 16 CZs. The results are also summarized in the attached spreadsheet.



Annual Savings_Fan Delay ET11SCE1130.:

APPENDIX F - TECHNOLOGY TEST CENTERS

Southern California Edison's (SCE) Technology Test Centers (TTC) are a collection of technology assessment laboratories specializing in testing the performance of integrated demand side management (IDSM) strategies for SCE's energy efficiency (EE), demand response (DR), and Codes and Standards (C&S) programs. Located in Irwindale, CA, TTC is comprised of four centers focused on distinct energy end uses: Heating, Ventilating, and Air Conditioning Technology Test Center (HTTC), Refrigeration Technology Test Center (RTTC), Lighting Technology Test Center (LTTC), and Zero Net Energy Technology Test Center (ZTTC), which is in development.

By conducting independent lab testing and analysis, TTC widens the scope of available IDSM solutions with verified performance and efficiency. TTC tests are thorough and repeatable, and conducted in realistic, impartial, and consistent laboratory environments to ensure the best quality results and recommendations.

The Design and Engineering Services (DES) group of SCE's Customer Service Business Unit manages TTC as a sub-element of the Emerging Technologies program.

HEATING, VENTILATION, AND AIR CONDITIONING TECHNOLOGY TEST CENTER

Heating, Ventilation, and Air Conditioning Technology Test Center (HTTC) evaluates the latest residential and commercial heating, ventilation, and air conditioning equipment. By testing systems and strategies in controlled environment chambers capable of surpassing industry standards and producing realistic climatic conditions, the HTTC can help EE program designers, customers, and the industry make informed HVAC design and specification decisions.

RESPONSIBILITIES

Key responsibilities include:

- **Testing:** HTTC tests HVAC equipment in support of California's statewide Emerging Technologies, Codes and Standards, and Demand Response. Testing capabilities include:
 - Packaged units (up to 7.5 tons)
 - Split systems
 - Control systems
 - Fault detection and diagnostic systems (FDD)
- **Evaluation:** HTTC evaluates the latest residential and commercial heating, ventilation, and air conditioning equipment to provide customers with the information necessary to make informed equipment purchasing decisions.
- **Equipment Efficiency Enhancement:** With funding support from statewide programs and research grants, HTTC works with manufacturers, state, and federal agencies to improve EE regulations addressing HVAC equipment.

TEST CHAMBERS AND EQUIPMENT

Test chambers and equipment include:

- **HVAC Indoor Test Chamber:** This 292 square foot test chamber provides thermal conditions typically found in air-conditioned spaces of residential and commercial buildings, where maintaining desirable human comfort is critical. It is used to collect precise data on temperature, airflow, and humidity in order to test various cooling strategies.
- **HVAC Outdoor Test Chamber:** This 250 square foot test chamber is used to replicate outdoor weather conditions, and to examine how air conditioning units respond under realistic climatic conditions. Temperatures can be maintained as high as 130°F.

REFERENCES

- 1 American Society of Heating, Refrigeration, and Air-Conditioning Engineers (2009). Methods of Testing for Rating Unitary Air-Conditioning and Heat Pump Equipment, Standard 37.
- 2 Air-Conditioning, Heating, and Refrigeration Institute (2008). Performance Rating of Unitary Air-Conditioning and Air-Source Heat Pump Equipment, Standard 210/240.
- 3 American Society of Heating, Refrigeration, and Air-Conditioning Engineers (2005). Fundamentals Handbook. Psychrometrics, Ch. 6.
- 4 National Institute of Standards and Technology, NIST, (1994). Guidelines for Evaluating and Expressing the Uncertainty of NIST Measurement Results. Technical Note 1297.